Undergraduate's Thesis

Sensitivity of Baffin Bay to exchanges through its gateway straits

by

Chuanshuai Fu - Department of Physics, East China Normal University, China

Supervisor:

Paul G. Myers - Department of Earth and Atmospheric Sciences, Faculty of Science, University of Alberta, Canada

Responsible teacher:

E Wu - Department of Physics, East China Normal University, China

Abstract

Baffin Bay has undergone major changes within recent years. We evaluate the exchanges through the gateway straits, to find out how the physical processes might influence the oceanic variability in Baffin Bay. Numerical output data from ANHA12 (A regional configuration of the coupled ocean-sea ice model NEMO at 1/12° resolution, covering the Arctic and the Northern Hemisphere Atlantic) are utilised to do the simulations for analysis. Firstly, we present that the ocean modelling transports are in good agreement with the corresponding observations, the correlations between the volume, freshwater and heat transports at different straits, as well as the annual variability and interannual variability for each. Secondly, we observe the two flow reversals at Davis Strait and Nares Strait, so we break down the analysis per water mass. At Davis Strait, the first one from November 2010 to January 2011 is caused by the reinforced northward WGSW and WGIW and diminished southward AW. The second one in December 2017 is due to the exceptional augmentation of WGIW. At Nares Strait, they are the result of a dominated northward AW. They could be driven by the elevation difference, the density distribution and baroclinic pressure gradients between the Baffin Bay and the Arctic Ocean or the North Atlantic Ocean. Lastly, we identify that Baffin Bay has become fresher and warmer from 2002 to 2010 based on the changes of freshwater content and heat content.

Keywords: Baffin Bay, Gateway Straits, Transports, Contents, Water Masses, Flow Reversal

Acknowledgement

A special gratitude to my supervisor, Paul G. Myers, who offered me an interesting project that I could put my passion and thoughts into it. Writing a thesis is more fun and fulfilling with his feedback, encouragement, and patience in guiding me through some details, especially with my writing. You are no doubt a real role model to me! I appreciate it that my responsible teacher E Wu decided to support my requirement to have Prof. Myers as my thesis supervisor, even through I need to translate it into a Mandarin version as well. Oh, no!

Thank you for my parents providing me a quiet environment and feeding me so well every single day during the self-quarantine at home, so that I have the inspiration and energy to do my work. Gain some weights but luckily don't need to worry about how to shed some pounds so far. Will keep you being proud of me! It takes my mind off things when the time spent with my childhood friends and my neighbor twins, like going out to the beach, having afternoon tea in tea houses, hanging around in our hometown and playing games from time to time. I am also thankful to my buddies Arthur, Steve and Jyoti, who always believe in me and show their support. Having discussions with you lights up my world in the darkest time!

The wonderful research experience last summer is a highlight in my university life. I will always remember the good old days with my awesome lab members, domestic and international interns, my host family and those friendly Canadians in Edmonton. However, never let the memories be greater than my dreams!

Lastly, I have to admit that I am also impressed with Adam's hard work, perseverance and intelligence. Ok, stay humble, but he definitely deserves the most credits for this thesis. Just stop watching too much cartoons! It is not the best solution when facing an uphill battle…

Contents

Lists of Tables

Lists of Figures

1. Background

1.1. Baffin Bay

Baffin Bay is a semi-enclosed Mediterranean sea composed of a flat-bottomed central basin of over 2300m depth, the steep-sided continental shelf off Baffin Island on the western periphery, and a relatively wide shelf on its eastern Greenland side, connecting the polar Arctic Ocean and sub-polar North Atlantic Ocean through its gateway straits (Fissel, Lemon and Birch, 1982; Tang et al., 2004). Therefore, the waters consist of Arctic water, Atlantic water and meltwater from the Greenland ice sheet. The Arctic inflow has an on-going chilling and freshening effect on Baffin Bay since it is the main source of cold and fresh water. The relatively warm and saline Atlantic water flows into Baffin Bay as currents through Davis Strait alleviates and stabilizes the effect (Zweng and Münchow, 2006). The glacial meltwater is greatly influenced by subpolar climatic variation, and it has potential positive feedback to Baffin Bay heat content on the eastern Baffin Bay shelf (Castro de la Guardia, Hu and Myers, 2015). In addition to thermohaline intrusion, Baffin Bay is a vibrant marine system with stratification and mixing, convection and cyclonic circulation, as well as biochemical processes. Validating the sensitivity is crucial to explore the dynamic of the system, which has significant implications for adjacent seas and global climate.

1.2. Davis Strait

Exchanges through Davis Strait are mostly two-way all year around. On the east side of Davis Strait, the warm (2~7 ℃), salty (34.5~35 psu) and persistent Atlantic-origin West Greenland Slope Current (WGSC) enters Baffin Bay at depths between 200m to 600m above the upper slope (Curry et al., 2011, 2014). Along the slope heading northward to Smith Sound, part of the current turns around, a branch flows cyclonically around the northern Baffin basin attributed to topographic steering, and lastly joins the southward flowing Baffin Island Current (BIC) (Figure 1.1). The other comparatively low-salinity current called the West Greenland Current (WGC) appears at the subsurface over the Greenland shelf with the depths ranging from 30m to 200m during the summer and early autumn months (Curry et al., 2011, 2014). Both the WGSC and WGC bring a large amount of heat and salt into Baffin Bay through the east side of Davis Strait. This, to a certain extent, contributes to the periods of nearly ice-free conditions in Baffin Bay from July to November. In general, the net outflow of Baffin Bay is a complex combination of cold, fresh liquid waters from the Arctic Ocean passing through the CAA, glacial river discharge from the CAA and Greenland, as well as drifting sea ice and icebergs. Transports are estimated as -1.6 ± 0.2 Sv in volume, -93 ± 6 mSv in liquid freshwater equivalent and -10 ± 1 mSv in sea ice, 2004-10 (Curry et al., 2011, 2014).

1.3. CAA

The Canadian Arctic Archipelago (CAA) is considered as the main pathway for the Arctic Ocean waters to flow into Baffin Bay through three entries. From North to South, they are Smith South via Nares Strait (500km long, 40km wide, sill at ~250m), Jones Sound via Cardigan Strait and Hell Gate (30km wide, sill at ~120m) and Lancaster Sound at the east end of Parry Channel via Barrow Strait (55km wide, sill at ~125m) (Tang et al., 2004) . These colder and fresher Arctic inflows meet together and form the

broad, surface-intensified Baffin Island Current (BIC), then travel southward along the western shelf as a dominating part of cyclonic circulation within Baffin Bay, ultimately exiting via the west side of Davis Strait (330km wide, sill at <640m) to the Labrador Sea (Cuny, Rhines and Kwok, 2005; Zweng and Münchow, 2006; Curry et al., 2014). Therefore, Baffin Bay plays a buffer role in the transportation and transition of the Arctic waters between CAA and the Labrador Sea.

1.3.1. Nares Strait

Nares Strait is a long, narrow conduit with basins and channels bounded by the Lincoln sea of the Arctic Ocean on the north, Baffin Bay on the south, Greenland to the east, and Ellesmere Island in the CAA to the west. Southward atmospheric forcing along the strait channelled by steep terrain has a great impact on freshwater and heat flux and ice advection (Samelson et al., 2006, 2008). The flow is forced by both wind and along-channel pressure gradient when the sea ice is mobile, whereas the effect of the wind surface stress weakens or even disappears when applied over the ice-covered ocean (Rabe et al., 2012). Therefore, the duration of ice arches from December to June across Smith Sound and Robeson Channel severely impair the dynamic of volume, freshwater and heat transport and prevent ice motion into and out of the strait (Münchow, 2016). However, the sea ice distribution in Nares Strait has been erratic in years when ice arches fail to form, resulting in year-round drifting sea ice and much more open water flux (Ryan, 2017). Consequently, the seasonal and interannual variability in transports would exert perturbance to the freshwater and heat storage within Baffin Bay. An observational estimate at mean subtidal volume and liquid freshwater fluxes and ice advection through Nares Strait are -0.87 ± 0.10 Sv, -43 ± 7.5 mSv and -8 ± 2 mSv from 2003 to 2009, respectively (Shroyer et al., 2015; Münchow, 2016).

1.3.2. Barrow Strait

Barrow Strait, as the southern-most passage, is the optimum location where long-term mooring observational data are collected, in order to calculate the volume and freshwater transport through Lancaster Sound entering into Baffin Bay. Results from Prinsenberg et al. (2009) show that mean volume flux through Lancaster Sound is roughly -0.7 Sv over an eight-year period (1998-2006), and from Peterson et al. (2012) is -0.46 Sv (-32 mSv for freshwater flux) through a thirteen-year time series (1998-2011). Prinsenberg et al. (2009) also presented a strong correlation between the volume transport through Barrow Strait and the northeastward alongshore winds in the Beaufort Sea, which determine the sea surface height difference between the Arctic Ocean and Baffin Bay, but it doesn't take effect in winter as revealed by Lu et al., (2014). Westward flow through Barrow Strait is restrained, and then recirculates towards the south because of the topography (a sill located at Barrow Strait) and salinity stratification (Wang et al., 2012). In terms of Cardigan Strait and Hell Gate, the throughflow is uniform in the middle depths but sheared close to surface and seafloor, estimated of -0.3 Sv in total volume (Melling et al., 2008). Two-thirds of the freshwater export from the Arctic into the North Atlantic is via the CAA and Baffin Bay (Aksenov et al., 2010). Doing research on how and in what form it is delivered in correspondence

with oceanic and atmospheric variability is vital for studying changes of the thermohaline circulation in both Baffin Bay and the North Atlantic.

1.4. Thesis Objectives

One of the objectives of my research is to compare the observational findings and ocean modelling results**.** The difficulties would be the sparse and limited observations due to the harsh weather conditions and inaccessible locations. Besides, modelling the exchanges of gateway straits in CAA is a challenging task on account of the complicated bathymetry and narrowness of the transects (Wekerle et al., 2013). However, in conjunction with the measurements in key hydrographic sections, numerical ocean modelling provides us with a useful tool to characterize and corroborate the temporal and spatial variability and thus better predict ocean evolution in the future. Other purposes in this thesis are as follows:

- The inner links among the volume, freshwater and heat transports will be studied, and different water masses will be taken into account individually.
- The intercomparison and interaction of transports through different cross sections are worth investigating.
- The physical dynamic responses of Baffin Bay to the exchanges through its gateway straits.

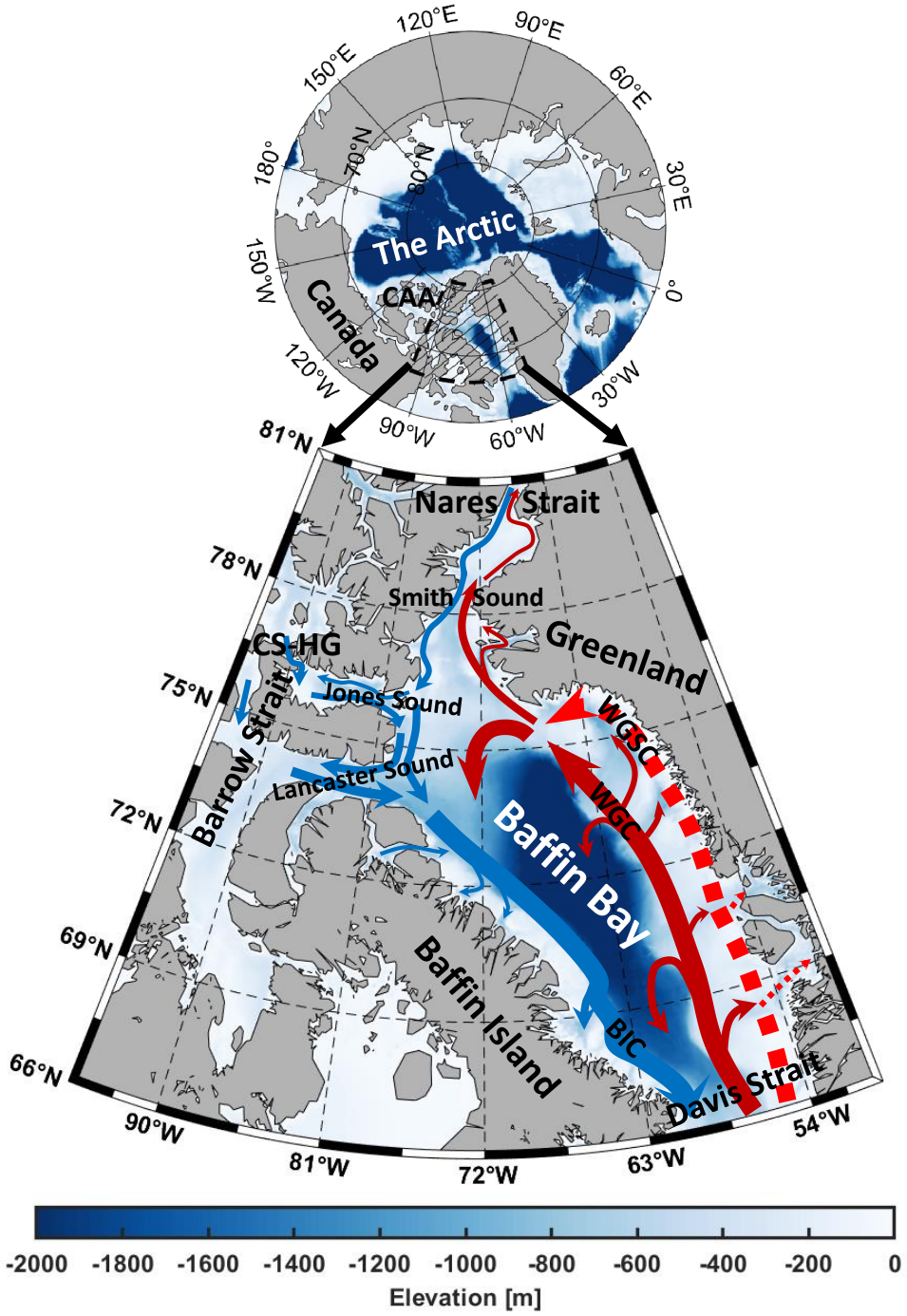

Figure 1.1. Maps of the Arctic Ocean surrounded by lands and the zoomed-in study area, demonstrating the general circulation and the regional bathymetry within Baffin Bay. The locations of the gateway straits and the northern CAA entrances into Baffin Bay are indicated. CAA: Canadian Arctic Archipelago; BIC: Baffin Island Current (blue line); WGC: West Greenland Current (dark red line); WGSC: West Greenland Shelf Current (red dashed line).

2. Numerical Methods

2.1. Numerical Model

In this study, we will use a state-of-art modelling framework called Nucleus for European Modelling of the Ocean version 3.4 (NEMO v3.4). Two major components of it are extensively used in physical oceanography research, one is the three-dimensional, eddy-permitting and primitive-equation ocean general circulation model Oc´ean PArall´elis´e (OPA), the other one is the sea ice model Louvain-la-neuve Ice Model version 2 (LIM2) with a modified elastic-viscous-plastic ice rheology, both including thermodynamic and dynamic processes (Fichefet and Maqueda, 1997; Hunke and Dukowicz, 1997; Madec and the NEMO team, 2008).

A staggered Arakawa C-grid for spatial discretization and numerical algorithms is widely used in NEMO due to its favorable conservation properties (Mesinger and Arakawa, 1976), whereby the variables are stored at different points in the unit cell of space domain (Figure 2.1). Scalar variables like temperature (T), salinity (S), pressure (p), and density (ρ) are displayed on the red T points; Meridional (v), zonal (u) and vertical (w) velocities are located on the green V points, blue T points and purple W points, respectively; The relative vorticity (ζ), planetary vorticity (f) and the barotropic stream function (ψ) are represented at the gold F points. All the points have a specific integer indexing in order to be computed in the code. The arrangement of variables is consistent in the three directions. The skeleton of the model grid is defined by two horizontal scale factors (e1, e2) and a vertical scale factor (e3) (Madec and the NEMO team, 2008).

A sub-domain configuration of the interactively coupled ocean-sea ice model NEMO covering the Arctic and the Northern Hemisphere Atlantic (ANHA) was applied to carry out the numerical simulations. The model mesh is extracted from the global ORCA tripolar grid, 1632*2400 grid points at each horizontal level, with a resolution of 1/12° (hereafter ANHA12) (Figure 2.2). The highest horizontal resolution is ~1.93km in Dease Strait, where it is near the artificial pole over northern Canada, while the lowest resolution is ~9.3km at the equator. The horizontal resolution in Baffin Bay is about 3.5km at gateway straits in northeastern CAA decreasing to 4.5km at Davis Strait. The vertical coordinates are 50 geopotential levels with the largest depth at 5727.92m, but which level needs to be set up depends on the depth of the cross section or the depth range we would like to look at. Higher resolution is applied to the upper ocean (<2m resolution for top 10m) with layer thickness going up from 1.05m at the surface to 453.14m at the last level in a gradient manner. The continental area is set to be zero. The bathymetry stems from the 1 arc-minute global relief model of Earth's surface (ETOPO1) built from NOAA dataset (Grivault, Hu and Myers, 2018), and the bottom topography (seafloor) is significantly improved by using partial steps (Bernard et al., 2006).

The integration of our numerical simulation starts from January 2002 to the end of December 2018 with 5-day average output. The initial conditions, including 3D ocean fields (temperature, salinity, zonal and meridional velocities) as well as 2D sea surface height and sea ice fields (sea ice concentration and thickness), are obtained from the GLobal Ocean ReanalYsis and Simulations 2 version 3 (GLORYS2v3) produced by Mercator Ocean (Masina et al., 2017; Hu et al., 2018). There are two open boundaries for ANHA12, one is close to Bering Strait in the Pacific Ocean and the other one aligns

at 20°S across the Atlantic Ocean. Open boundary conditions (temperature, salinity and horizontal ocean velocities) are also derived from GLORYS2v3 dataset (Hu, Myers and Lu, 2019). The high temporal (hourly) and spatial (33km) resolution atmospheric forcing acting on the sea surface, including 10-m wind, 2-m temperature, and specific humidity, total precipitation as well as surface downwelling shortwave and longwave radiative fluxes, are taken from the Canadian Meteorological Centre's (CMC) Global Deterministic Prediction System (GDPS) ReForcasts (CGRF) dataset (Smith et al., 2014; Hu et al., 2018). These forcing fields are linearly remapped onto the model grid, significantly increasing the reliability of evaluation and the precision of prediction in our model.

The model time step for ANHA12 is 180s. No temperature and salinity are restored so that the model evolves with no constraints in time so as to not damp the freshwater signals. Tides are not taken into consideration in the numerical experiment since we will only focus on representing the large-scale processes (Ridenour et al., 2019).

2.2. Transport and Content

The volume, freshwater and heat transports could reflect the seawater thermodynamic and dynamic processes in the coupled ocean-sea ice model. The transport in the gateway straits becomes a measure of the degree of interactions between two bodies of water. The exchange through those gateway straits has been fluctuating over the years, possibly showing some regular patterns and anomalous features. Therefore, calculating them with numerical modelling quantitatively is one of the achievable ways not only to visualize and analyze these shifts, but also aid in discovering the mechanisms behind the shifts, which would deepen our understanding to their potential impacts to Baffin Bay.

The volume transport depends on the cross-strait velocity and section area. The freshwater and heat transports derive from the volume transport with the salinity and temperature being considered individually. The freshwater transport is equivalent to zero-salinity water flux that is added to or deducted from the volume transport in reference salinity to reach the sample salinity. The heat transport is equal to the extra or deficient heat flux of volume transport in sample temperature than the heat contained in the same amount of volume transport in reference temperature. The freshwater and heat transports must be combined to better understand the variability of thermohaline intrusion into Baffin Bay. They can be computed from 5-day mean output from the numerical model as follows:

The volume transport (Sv, $1Sv = 10^6 m^3/s$):

$$T_{Vol} = \sum_{i=1}^{n} v_i A_i$$

where v_i is the cross-strait seawater velocity at each model grid cell (m/s), A_i is the area of single model grid cell (m^2), n is the number of grid cells in the cross section.

The freshwater transport (mSv, $1mSv = 10^3 m^3/s$):

$$T_{FW} = \sum_{i=1}^{n} v_i A_i \left(\frac{S_{ref} - S_i}{S_{ref}}\right)$$

The heat transport (kW or kJ/s):

$$T_H = \sum_{i=1}^{n} v_i A_i \rho_o C_p (\theta_i - \theta_{ref})$$

where S_i is the seawater salinity (psu), S_{ref} is the reference salinity (34.8 psu); θ_i is the seawater potential temperature (℃), θ_{ref} is the reference temperature (0 ℃); ρ_o is the reference density of the seawater (1,030 kg/m^3), C_p is the specific heat capacity of the seawater ($4.0 * 10^3\ J/(kg \cdot ℃)$).

The expected manifestations of the sensitivity to exchanges are the changes of the freshwater and heat content, which are counted within Baffin Bay enclosed by its gateway straits or Baffin Bay Box in the following study. The freshwater content in the domain is calculated by the amount of zero-salinity water required by the seawater volume in reference salinity to reach studied seawater sample salinity. The heat content is the heat storage discrepancy between the seawater volume in reference temperature and studied seawater sample.

The freshwater content (m^3):

$$V_{FW} = \int_0^V \left(\frac{S_{ref} - S_i}{S_{ref}}\right) dV = \iint_{-D}^{0} \left(\frac{S_{ref} - S_i}{S_{ref}}\right) dAdz$$

The heat content (kJ):

$$H = \int_0^V \rho_o C_p (\theta_i - \theta_{ref})\, dV = \iint_{-D}^{0} \rho_o C_p (\theta_i - \theta_{ref}) dAdz$$

where dA is the differential area of the horizontal domain (m^2). D is the largest depth of the domain (m), different depths will be applied to different straits.

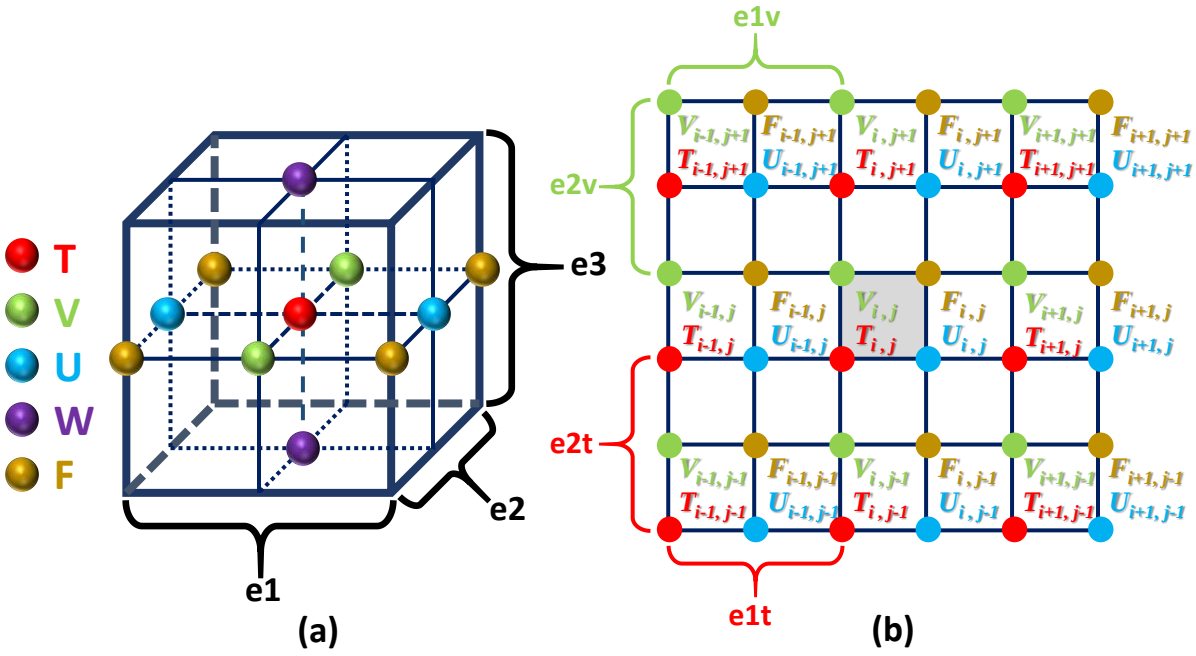

Figure 2.1. 3D cabinet perspective (a) and 2D top down view (b) of the variable arrangement in the NEMO mesh grid (Arakawa C-grid). The red T point in the cell center represents scalar points; The green V points, blue T points and purple W points in the center of each face indicate vector points; The gold F point in the center of each vertical edge stands for vorticity points. Three scale factors (e1, e2: horizontal; e3: vertical) define the size of each grid cell in (a). Horizonal integer indexing has been chosen as shown in (b). The T, V, U, F points having the same i- and j-indices are indicated by the dashed square. e1t, e2t is the length of T grid cell in the horizonal plane, and so on.

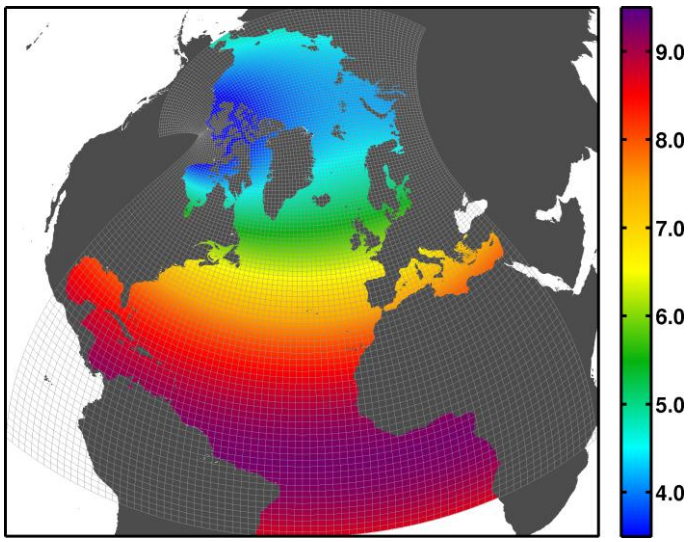

Figure 2.2. ANHA12 horizontal mesh (every 20 grids, color shows the resolution in kilometers). The singular point is moved to Dease Strait from the North Pole.

3. Transports in the Cross Sections (2002-2018)

3.1. Volume Transport

The net volume transport through Davis Strait from 2002 to 2018 is -1.51 ± 0.05 Sv (Figure 3.1a). From October 2004 to September 2010, the estimate in the model is -1.56 Sv, which is very close to the observation of -1.6 Sv from Curry *et al.*, (2014) based on the same time period (Table 3.1). The annual net southward transport goes down to -0.53 Sv in 2010, and then gradually increases back to near the average. The volume transport is comparatively lower from 2010 to 2014. On a monthly average, the maximum normally happens from October to December, but it has become more variable and unpredictable in recent years after 2010, in which year a flow reversal appears. Another reversal occurs in December 2017.

At Nares Strait, the net averaged volume transport over the whole model period is -0.89 ± 0.02 Sv (Figure 3.1b). The observations were taken from two periods, 2003-2006 and 2007-2009, with a mean volume flux of -0.87 Sv (Münchow, 2016). At the same time scale, the estimated mean in the model is -0.90 Sv, so the experimental result agrees well with the observational finding. The annual net southward transport maintains the same level until it drops to -0.39 Sv in 2010, then fluctuated around the average in the later years. The correlation coefficient between the Nares Strait and Davis Strait is quite high in the model with the value of 0.83 (Figure 3.4 ①). Like Davis Strait, the volume transport through Nares Strait flows in reverse in the same months in 2010 and 2017.

The net volume transport at Barrow Strait throughout the entire period is the lowest among the three straits, with an average transport of -0.68 ± 0.03 Sv (Figure 3.1c). The observational value of -0.7 Sv from Prinsenberg *et al.* (2009) is under the error range. The volume transport experiences a decreasing trend between 2002 to 2010 from -1.37Sv to -0.17 Sv, then rises to slightly above the average in the last year in the model. The timing of the annual maximum and minimum varies from year to year. The volume transport at Barrow Strait is more related to Davis Strait (0.90) than Nares Strait (0.50) (Figure 3.4 ②③).

3.2. Freshwater Transport

The net liquid freshwater transport through Davis Strait is southward for all years and months with an average of -92.0 ± 2.3 mSv (Figure 3.2a). The experimental result is in agreement with the observation of -93mSv in the literature (Curry *et al.*, 2014). The annual freshwater transport remains fairly stable but suddenly falls to -43.8 mSv in 2010, then it shows steady growth in the later years, peaking at -138.8 mSv in 2017. The annual cycle of freshwater transport in 2017 has an anomalous maximum of -220.4 mSv in February. The net liquid freshwater transport is moderately correlated to the volume transport (0.52; Figure 3.4 ⑩).

At Nares Strait, the average of the net liquid freshwater transport is -42.5 ± 1.2 mSv (Figure 3.2b). This coincides with the observation of -43 mSv from Münchow (2016). The freshwater transport remains stable and no significant trend is observed interannually. However, the fluctuation range is markedly greater within 2010 and 2017, in which years the freshwater transport flows northward going with the volume

transport in some months. This is consistent with the high correlation coefficient of 0.81 between freshwater transport and volume transport (Figure 3.4 ⑫). The freshwater transport is moderately related between Nares Strait and Davis Strait (0.44; Figure 3.4 ④).

The net liquid freshwater transport through Barrow Strait is higher than that of the Nares Strait with an average of -57.8 ± 2.5 mSv (Figure 3.2c), although the volume transport is comparatively lower. The freshwater transport decreases steadily between 2002 and 2010 from -78.9 mSv to -16.7 mSv, and then increases gradually to -85.0 mSv in 2018. Compared with the interannual variability with the coefficient of variability of 0.39, the annual variability is larger with the value of 0.54 (Table 3.2). The correlation between the freshwater and volume transport at Barrow Strait is considerably high with the correlation efficient of 0.89 (Figure 3.4 ⑭). The correlation coefficient between Barrow Strait and Davis Strait for freshwater transport is higher with the value of 0.60, than that of 0.22 between Barrow Strait and Nares Strait (Figure 3.4 ⑤⑥).

3.3. Heat Transport

The net heat transport through Davis Strait is significantly higher than Barrow Strait and Nares Strait with an average of 19.2 ± 0.9 TW (Figure 3.3a), which also fits well with the observation of 20 TW (Curry, Lee and Petrie, 2011). The timing of the yearly maximum and minimum are typically consistent from year to year, with the annual maximum heat inflow to Baffin Bay occurring in October-December (Autumn) and annual minimum in April-June (Spring). The interannual variability is substantially less variable than the annual variability, with an interannual standard deviation of 5.7 TW and an average annual standard deviation of 11.8 TW, as well as the interannual coefficient of variability of 0.30 and an average annual coefficient of variability of 0.67 (Table 3.2). The average monthly heat transport is the highest of all years in December 2010 with a spike of 70.5 TW. In recent years heat inflow becomes relatively less interannually. The correlation coefficient between heat transport and volume transport at Davis Strait is 0.45 (Figure 3.4 ⑪).

The net mean heat transport at Nares Strait is 3.57 ± 0.10 TW (Figure 3.3b). Annual heat transport does not change a lot until it sharply slumps to 1.86 TW in 2010, then shows an upward trend with a peak of 5.33 TW in 2015, followed by a gradual descent in later years. The relationship between the heat transport and volume transport is strongly negative with a correlation coefficient of -0.90 (Figure 3.4 ⑬). The heat transport at Nares Strait is moderately related to Davis Strait (-0.56; Figure 3.4 ⑦).

The net heat transport at Barrow Strait is comparable to that at Nares Strait with an average of 3.63 ± 0.17 TW (Figure 3.3c). There is a steady decline in heat transport between 2002 and 2010 from 7.75 TW to 1.00 TW. It remains stable for a few years but increases to the average level in 2015. The heat transport at Barrow Strait has an extremely strong link to its volume transport with the correlation coefficient of -0.98 (Figure 3.4 ⑮). However, its correlations to the heat transport at both Davis Strait and Nares Strait are not obvious with the respective coefficient of -0.14 and 0.16 (Figure 3.4 ⑧⑨).

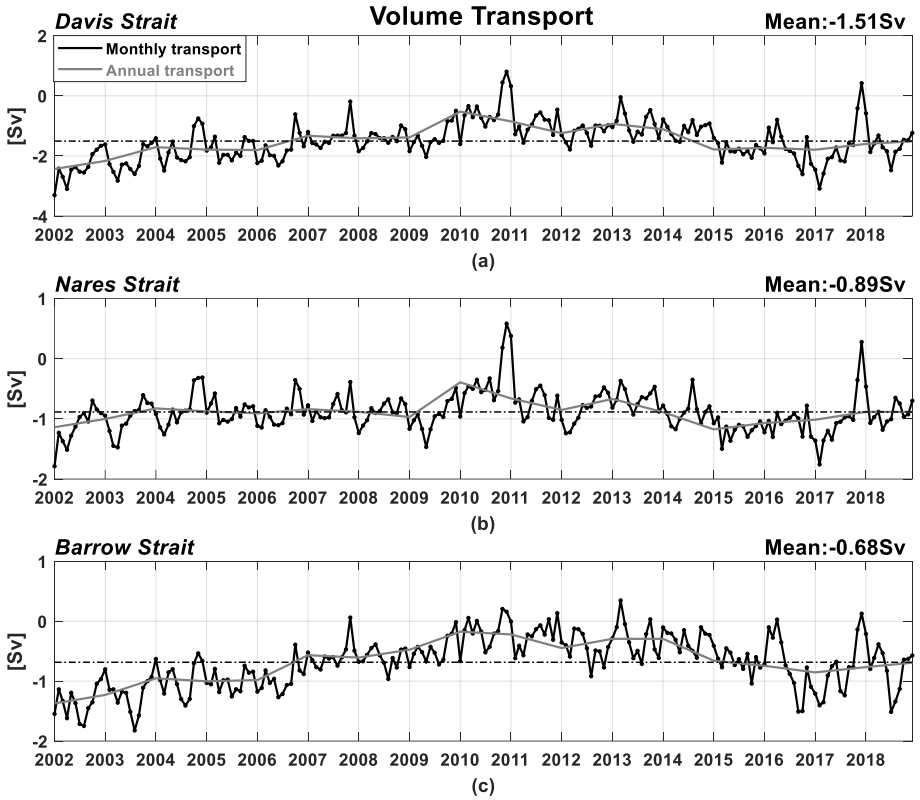

Figure 3.1. Volume transport for Davis Strait, Nares Strait and Barrow Strait from 2002 to 2018. They are shown on a monthly transport (black line) and annual transport (gray line). The dash-dotted line indicates the mean of volume transport over the whole model period. All transports are computed from the surface to the straits bottom. The sign refers to the direction rather than the magnitude, which is prescribed as a positive value means toward the Arctic Ocean, while a negative value means into the North Atlantic, i.e. transports are positive northwards and westwards.

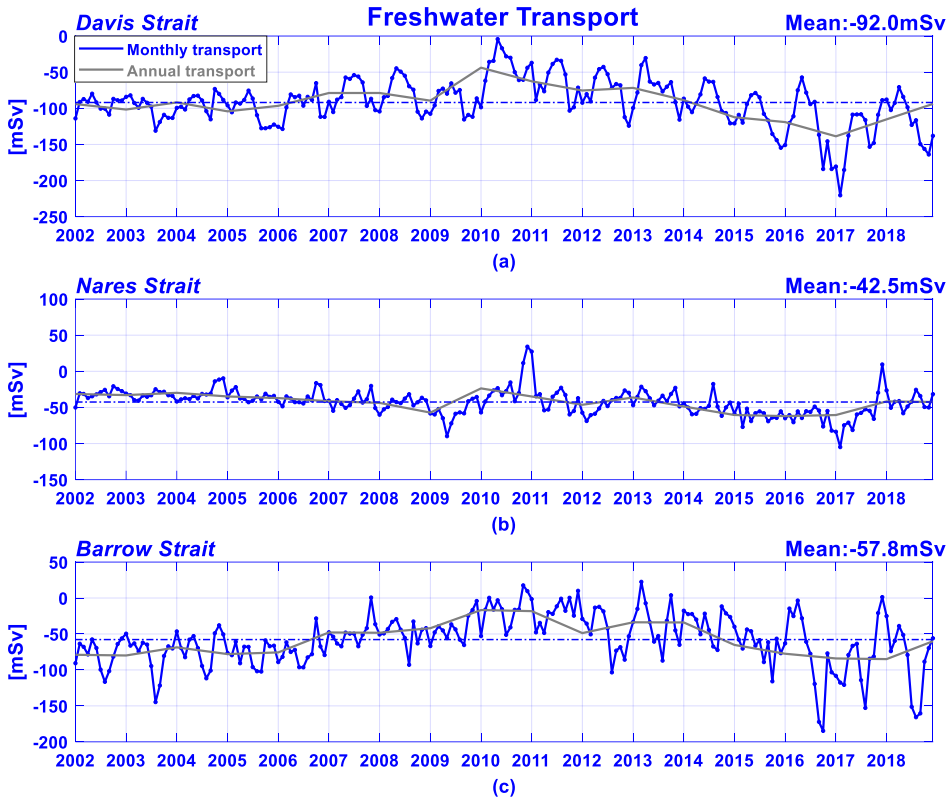

Figure 3.2. Freshwater transport (reference 34.8) for Davis Strait, Nares Strait and Barrow Strait from 2002 to 2018. They are shown on a monthly transport (blue line) and annual transport (gray line). The dash-dotted line indicates the mean of freshwater transport over the whole model period. All transports are computed from the surface to the straits bottom. The sign refers to the direction rather than the magnitude, which is prescribed as a positive value means toward the Arctic Ocean, while a negative value means into the North Atlantic, i.e. transports are positive northwards and westwards.

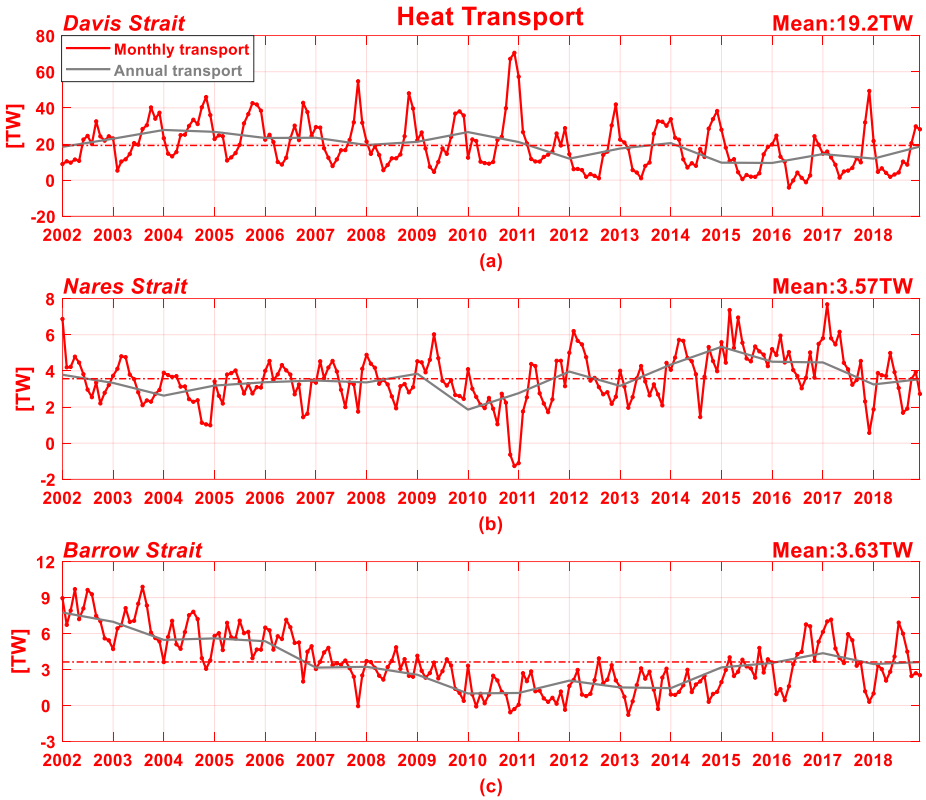

Figure 3.3. Heat transport (reference 0°C) for Davis Strait, Nares Strait and Barrow Strait from 2002 to 2018. They are shown on a monthly transport (red line) and annual transport (gray line). The dash-dotted line indicates the mean of heat transport over the whole model period. All transports are computed from the surface to the straits bottom. The sign refers to the direction rather than the magnitude, which is prescribed as a positive value means toward the Arctic Ocean, while a negative value means into the North Atlantic, i.e. transports are positive northwards and westwards.

Section Name	Time Period	Volume Transport (Sv)	Freshwater Transport (mSv)	Heat Transport (TW)	Source
Davis Strait	2002-2018	-1.51 ± 0.05	-92.0 ± 2.3	19.2 ± 0.9	ANHA12
	2004-2010	-1.56			ANHA12
	2004-2010	-1.6 ± 0.2	-93 ± 6	20 ± 9	Curry et al., 2014
Nares Strait	2002-2018	-0.89 ± 0.02	-42.5 ± 1.2	3.57 ± 0.10	ANHA12
	2003-2009	-0.90			ANHA12
	2003-2009	-0.87 ± 0.10	-43		Münchow, 2016
Barrow Strait	2002-2018	-0.68 ± 0.03	-57.8 ± 2.5	3.63 ± 0.17	ANHA12
	1998-2006	-0.7			Prinsenberg et al., 2012

Table 3.1. Summary of the volume, freshwater and heat transports through the Gateway Straits of Baffin Bay from ANHA12 and observations. The sign for transport is prescribed as a positive value means toward the Arctic Ocean, while a negative value means into the North Atlantic.

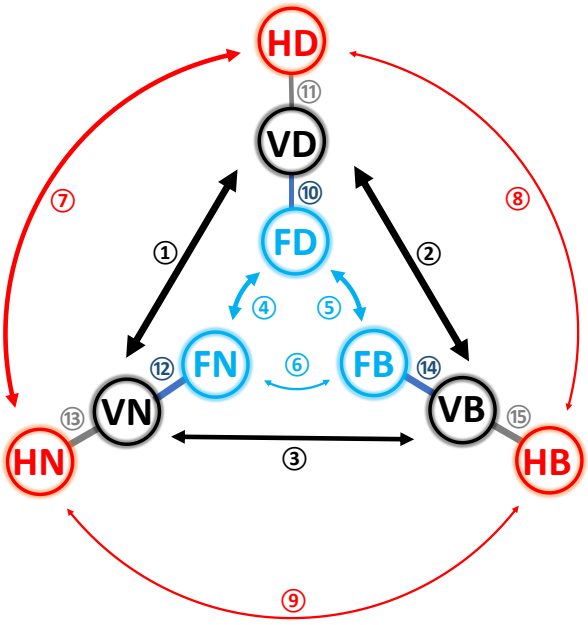

Figure 3.4. Correlations of the volume, freshwater and heat transport through the gateway straits in Baffin Bay. VD, FD and HD represent the Volume, Freshwater and Heat transport for Davis Strait respectively; VN, FN and HN stand for the Volume, Freshwater and Heat transport for Nares Strait respectively; VB, FB and HB mean the Volume, Freshwater and Heat transport for Barrow Strait respectively. Enclosed numbers are the correlation coefficients between the transports. ① = 0.83; ② = 0.90; ③ = 0.50; ④ = 0.44; ⑤ = 0.60; ⑥ = 0.22; ⑦ = -0.56; ⑧ = -0.14; ⑨ = 0.16; ⑩ = 0.52; ⑪ = 0.45; ⑫ = 0.81; ⑬ = -0.90; ⑭ = 0.89; ⑮ = -0.98. Three kinds of thickness of the connecting solid lines correspond to three ranges of strength of the association among the transports, which are simply categorized here. Thin line: 0.01 - 0.29, weak relationship; Thick line: 0.30 - 0.69, moderate relationship; The thickest line: 0.70 or higher, strong relationship. The negative sign denotes a negative relationship, otherwise it would be a positive relationship.

Transport		Volume			Freshwater			Heat		
Gateway Straits		DS	NS	BS	DS	NS	BS	DS	NS	BS
Standard Deviation	Annual average	0.45 Sv	0.26 Sv	0.27 Sv	23.1 mSv	12.4 mSv	26.6 mSv	11.8 TW	1.10 TW	1.30 TW
	Interannual	0.47 Sv	0.18 Sv	0.34 Sv	22.2 mSv	11.4 mSv	22.4 mSv	5.7 TW	0.79 TW	1.97 TW
Coefficient of Variability	Annual average	0.35	0.33	0.53	0.26	0.32	0.54	0.67	0.33	0.47
	Interannual	0.31	0.21	0.50	0.24	0.27	0.39	0.30	0.22	0.54
	Intra-annual	0.43	0.34	0.64	0.32	0.40	0.57	0.52	0.34	0.65

Table 3.2. Annual, interannual and intra-annual variability for the volume, freshwater and heat transports at its gateway straits of Baffin Bay. The standard deviation is a measure of the dispersion from the mean. The efficient of variability is the radio of the standard deviation divided by the mean. DS = Davis Strait; NS = Nares Strait; BS = Barrow Strait.

4. Gateway Straits

4.1. Davis Strait

4.1.1. Water Masses and Seasonal Changes

Due to the distinct properties of the currents through Davis Strait, according to the specific temperature and salinity ranges, four primary water masses are defined by Curry et al. (2014). They are Arctic Water (AW; $\theta \leqslant 1$ ℃; $S \leqslant 33.7$) flowing southward as the BIC at depths <300 m; Transitional Water (TrW; $\theta \leqslant 2$ ℃; S>33.7) normally found at depths >300 m; West Greenland Shelf Water (WGSW; $\theta < 7$ ℃; S<34.1) flowing northward as the WGC; West Greenland Irminger Water (WGIW; $\theta > 2$ ℃; S>34.1) flowing cyclonically as part of the WGSC. Each of these water masses has its own origin and a unique travelling path before flowing through Davis Strait. The annual variations of the seasonal average temperature, salinity and cross-strait velocity from 2004 to 2016 are presented in Figure 4.1 with the locations of four water masses indicated in the summer.

Seasonal atmospheric temperature variations have a significant effect on the annual temperature cycle in the upper ocean. The sea surface can obtain different amounts of heat from the sun with the change of seasons, which becomes a crucial factor to the distribution of the temperature in the cross section, such as AW and WGSW reach a maximum temperature during the summer. The higher temperature leads to the melt of sea ice, glacial runoff from West Greenland, even more precipitation in the region, the addition of freshwater decreases salinity and increases stratification.

The salinity stratification is clear in the upper 200m and the seawater is a lot fresher on the surface in summer and autumn in the annual cycle. From the surface to the sea bottom, the seawater in the cross section gets salter on account of density raising whereas the salinity of WGIW (Water mass above the east upper slope) is always the highest. Maximum temperature, salinity and northward velocity of the WGIW occurred in autumn, and the strength of it exerts a great influence on other surrounding water masses by interplaying and mixing at the boundary.

Exchanges through Davis Strait are two-way all year around. The bathymetry in strait causes stronger velocities along the edges and weaker velocities in the interior at depth. Although the vast majority of the southward flow appears over half the strait from Baffin Island, extending to ~150km, a fraction of it is also presented over the west Greenland slope, especially during winter and spring. The location of the core of southward flow moves in response to seasons. For instance, it moves to closer to the shelf of Baffin Island in the summer. Northward current is maximum in Autumn up to 15 cm/s, while the annual minimum velocity is in the spring. TrW is the largest water mass by area but flowing southward at quite a low speed.

4.1.2. 2010-2011 and 2010/12

From the analysis in section 3, first flow reversal through Davis Strait was found

from November 2010 to January 2011. To better understand the phenomenon, timeseries for volume, freshwater and heat transports at Davis Strait from January 2010 to December 2011 is shown on a 5-day mean transport (Figure 4.2). The simulated volume and freshwater transports crossing Davis Strait are -0.67 $\pm$ 0.07 Sv and -53.5 $\pm$ 2.9 mSv respectively, both quite lower than those over the whole model period, denoting less southward flow. It could be less seawater (AW or TrW) is transported from Baffin Bay to the Labrador Sea or more seawater (WGIW or WGSW) flows northwards into Baffin Bay during the period. The northward heat transport is a function of both cold seawater ($<$ 0℃) southwards and warm seawater ($>$ 0℃) northwards. The heat transport at Davis Strait of 2010-2011 is 24.6 $\pm$ 1.7 TW, 28% larger than 17-year model average, inferring either more cold seawater (AW or TrW) flows southwards or more warm seawater (WGIW or WGSW) goes northwards. Combined analyses above, an increased inflow of WGIW and/or WGSW during this period could explain the changes.

The correlation coefficient between the volume transport and heat transport is as high as 0.92 during the red-painted period, whereas only 0.45 for the blue-painted period (Figure 4.2). The high relevance between them during the autumn months is consistent with the timing of the seasonal maximum of WGIW. The data of the transport through Davis Strait in December 2010 were selected for further investigation (Figure 4.3). It clearly shows that WGIW becomes stronger and wider with larger northward velocity, containing a huge amount of heat and salt, hence pushing the boundaries of other ambient water masses. Owing to the much higher salinity in the core, even larger than the reference salinity of 34.8, the fact that more salty seawater flowing northwards is equivalent to that more freshwater transports southward. This is compatible with that the volume transport is more associated with heat transport rather than freshwater transport during the period. WGSW also flows into Baffin Bay at large speed, compared with WGIW, it carries less heat but more freshwater.

To further study the correlation between the volume transport and heat transport in December, seawater volume and heat content through Davis Strait for the months from 2002 to 2018 are calculated (Figure 4.4). The variability in December for seawater volume is quite large with an intra-monthly coefficient of variability of 0.73, whereas it is 0.35 for heat content. The seawater volume reaches a bottom of around -2500 km^3 in 2004, followed by an increase back to its initial state in 2006. It experiences a steady decline since then and switches its direction in 2010, reaching approximately 2000 km^3. Then it shows an upward trend but suddenly has another reversal in 2017, half volume of that in 2010.

The seawater volume and heat content in December for the model years are correlated at 0.84. Nevertheless, heat content through Davis Strait in December does not show a clear trend except for notably larger portions in December of 2010 and 2017, and heat content in December 2010 is twice as much as the average. Therefore, northward seawater volume through Davis Strait has

brought a great deal of heat content into Baffin Bay.

4.2. Nares Strait

4.2.1. 2010-2011 and 2010/12

Likewise, timeseries for volume, freshwater and heat transports at Nares Strait from January 2010 to December 2011 is shown on a 5-day mean transport (Figure 4.5). The volume, freshwater and heat transports passing through Nares Strait during the period are -0.52 $\pm$ 0.04 Sv, -28.5 $\pm$ 2.5 mSv, 2.29 $\pm$ 0.17 TW respectively, roughly two-third of those over the whole model years. The freshwater transport represents nearly the same variability as the volume transport, with a statistically significant correlation coefficient of 0.98. On the contrary, the correlation between the heat transport and volume transport is strongly negative with r = -0.96. A reflux of volume transport also appears at Nares Strait over the same period. There can be a driving mechanism enhancing cyclonical circulation in Baffin Bay, then leading to the flow reversals simultaneously at gateway straits, so how the flow reversal might affect at Nares Strait would be studied here.

The transport through Nares Strait is predominantly southward over two years, bringing an abundance of cold (< 0℃) and fresh (< 34.8 psu) seawater from the Arctic to Baffin Bay (Figure 4.6a). The two-year averaged temperature and salinity at Nares Strait are clearly stratified by the means of increasing from the surface to the strait bottom. The northward volume transport from November 2010 to January 2011 results in the freshwater transport back to the Arctic Ocean, primarily through the upper halfway strait. As part of West Greenland Slope Current (WGSC) and West Greenland Current (WGC), WGIW and WGSW keep heading northward even to Smith Sound along the slope of Greenland. The properties of water masses have been diluted after mixing with the melting sea ice and glacial runoff in Baffin Bay, they could become fairly cold and fresh and transform into AW or TrW when reaching Nares Strait (Figure 4.6b). The increased cold (< 0℃) northward seawater is accounted for the counterturn of heat transport. The core temperature at the middle depth of Nares Strait is only slightly higher than 0℃ in December 2010, so this portion of seawater is not strong enough to make a difference to the overall heat transport direction.

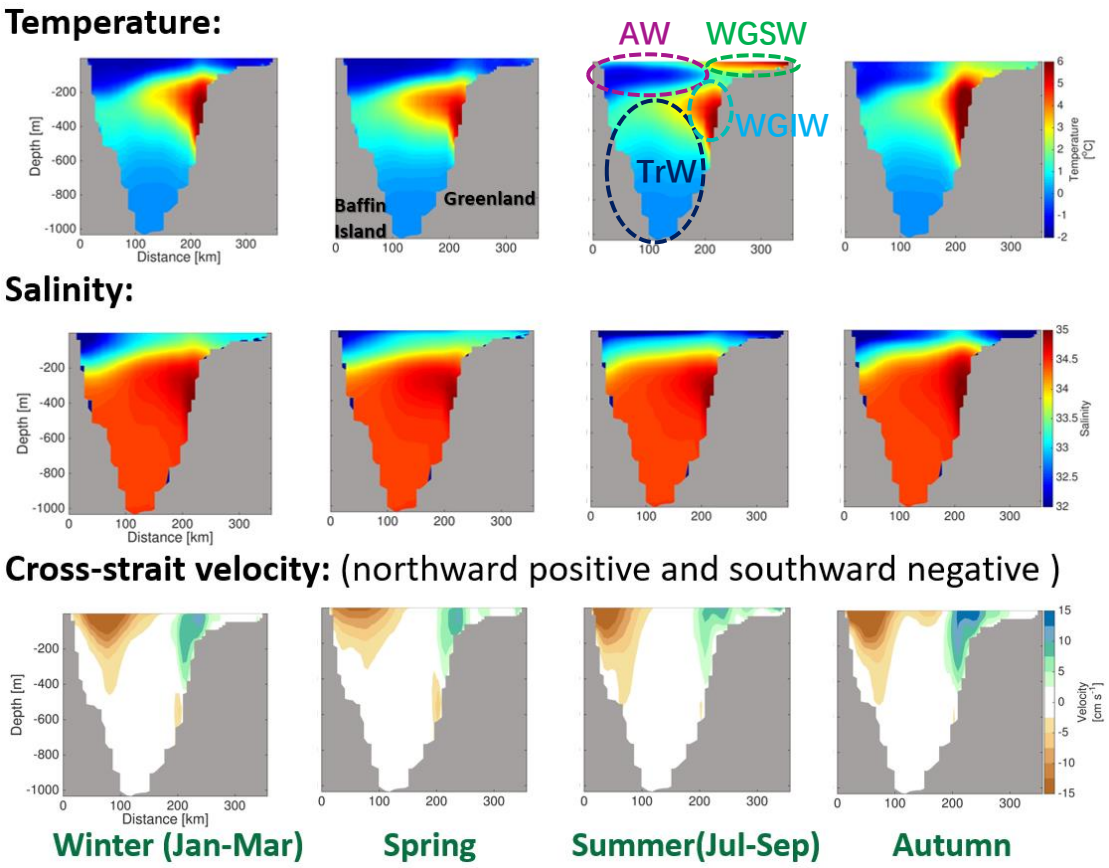

Figure 4.1. Seasonal climatology of temperature, salinity and cross-strait velocity, representing heat and salt flux across Davis Strait over the years from 2004 to 2016. Four primary water masses are divided by different temperature and salinity ranges.

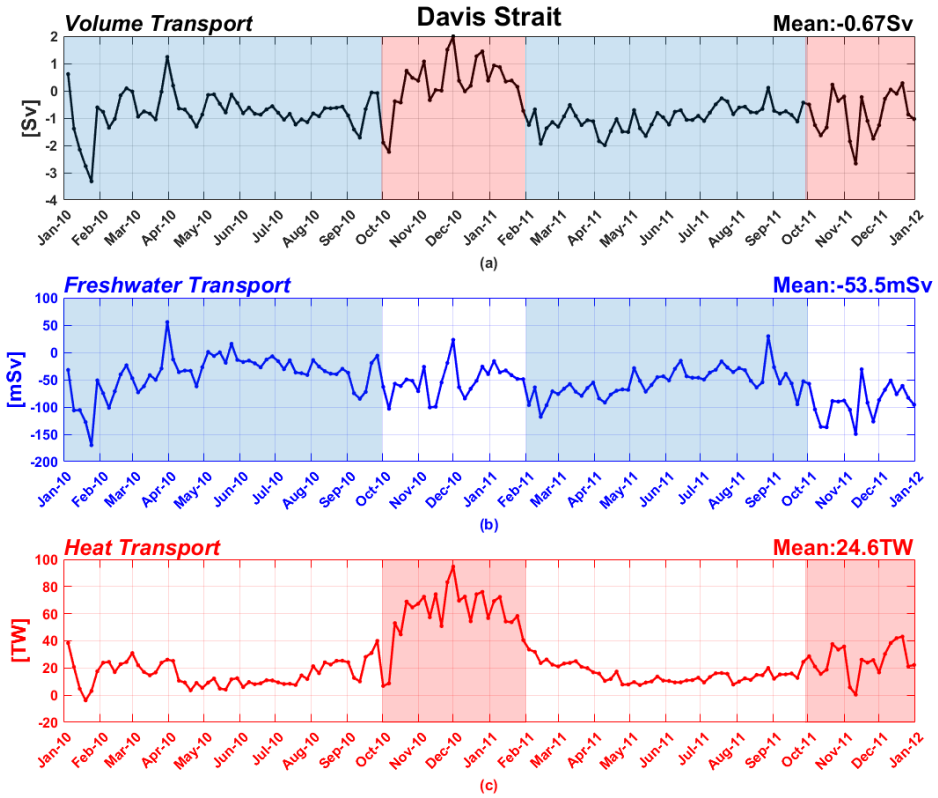

Figure 4.2. Volume, freshwater and heat transports for Davis Strait from January 2010 to December 2011. They are shown on a 5-day mean transport. All transports are computed from the surface to the straits bottom. The sign refers to the direction rather than the magnitude, which is prescribed as a positive value means toward the Arctic Ocean, while a negative value means into the North Atlantic, i.e. transports are positive northwards and westwards.

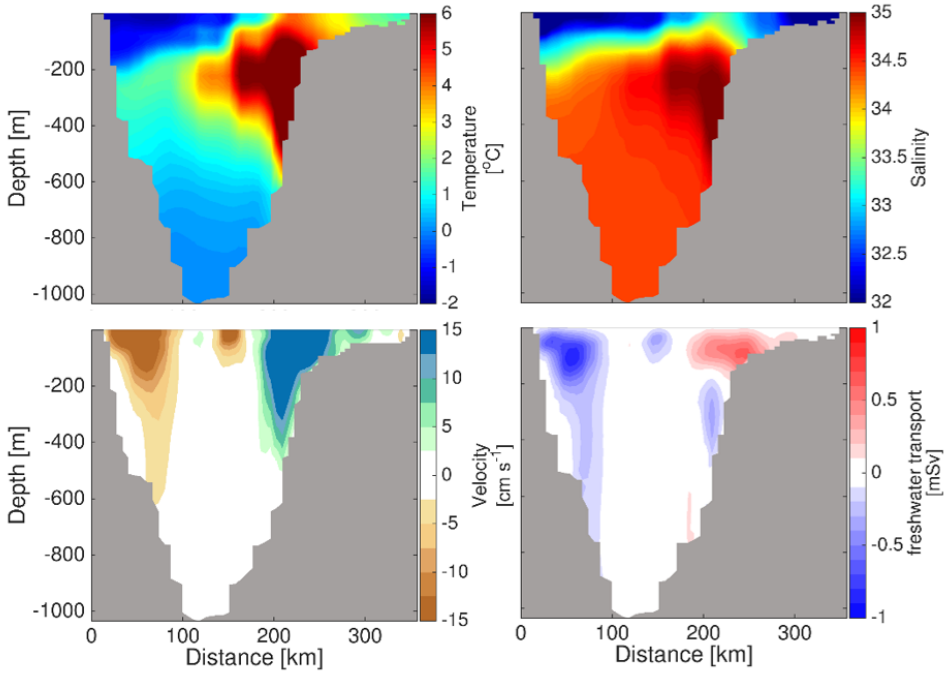

Figure 4.3. Monthly average of temperature, salinity, cross-strait velocity and freshwater transport at Davis Strait in December 2010.

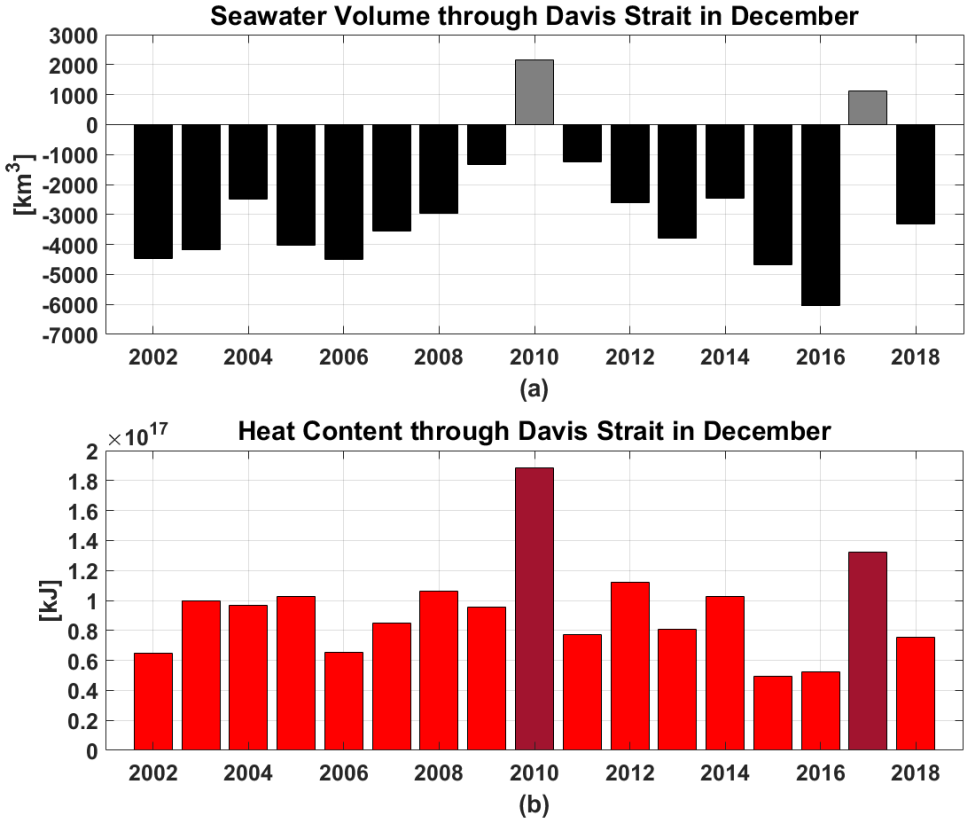

Figure 4.4. Seawater volume (a) and heat content (b) through Davis Strait in December from 2002 to 2018, in which 2010 and 2017 are emphasized by using different stand-out colors.

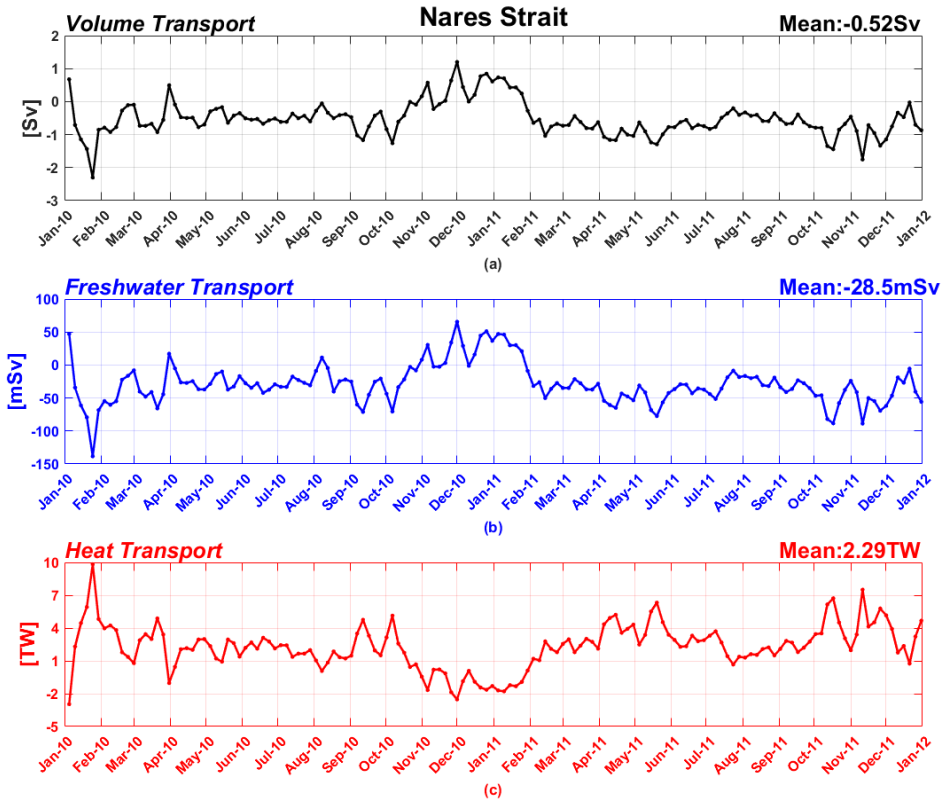

Figure 4.5. Volume, freshwater and heat transports for Nares Strait from January 2010 to December 2011. They are shown on a 5-day mean transport. All transports are computed from the surface to the straits bottom. The sign refers to the direction rather than the magnitude, which is prescribed as a positive value means toward the Arctic Ocean, while a negative value means into the North Atlantic, i.e. transports are positive northwards and westwards.

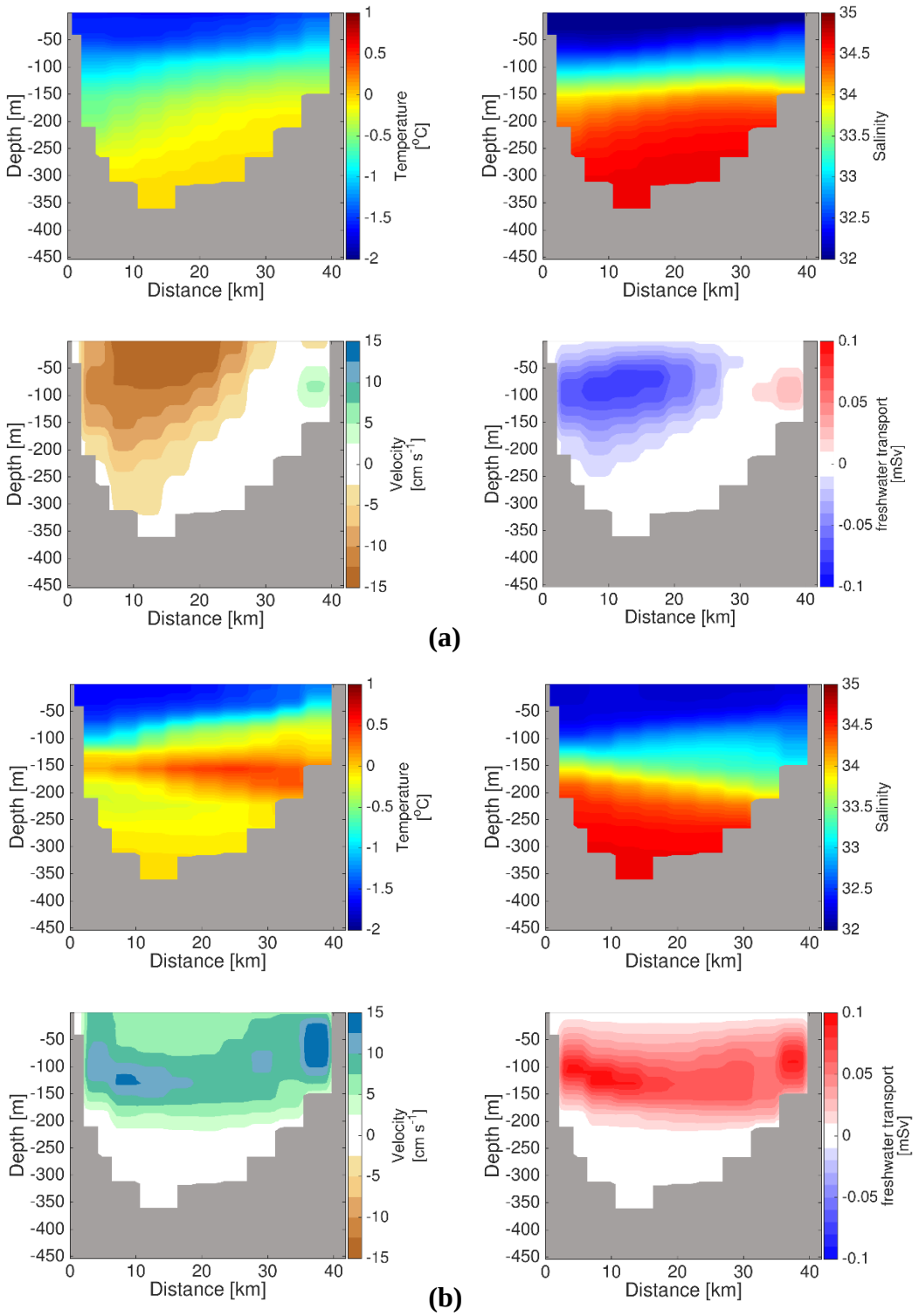

Figure 4.6. Two-year average of temperature, salinity, cross-strait velocity and freshwater transport at Nares Strait from January 2010 to December 2011 (a); Monthly average of temperature, salinity, cross-strait velocity and freshwater transport at Nares Strait in December 2010 (b).

5. Water masses Fluxes

5.1. Arctic Water

The net AW volume transport is southward from beginning to end in the model, with the mean transport of -1.42 Sv (Figure 5.1a), accounting for 52% of the total volume transport at Davis Strait (Figure 5.2a). The AW is the product of water mass that largely comes from the Arctic Ocean, passing through CAA passages and being modified in Baffin Bay until arriving at Davis Strait, so the variability of AW at Davis Strait is driven by the variability of the Arctic outflow. The annual variability is a lot more stable from 2002 to 2005 during the four-year period than the latter years (The average of annual AW volume transport standard deviation: 0.18 Sv versus 0.4 Sv; Annual average for the coefficient of variability: 0.10 versus 0.30). Annual variability in AW has the tendency to be southward minimum in the summer (April-June), then ascend to reach peak transport during autumn (October-December). The range gap in AW transports between the minimum and maximum during the whole model period is as high as 2.50 Sv. The interannual variability coefficient is 0.16, reflecting the relatively steady transport on a yearly basis. AW contains a large amount of freshwater and correlated with freshwater transport at 0.82.

At Nares Strait, the average AW volume transport in the experiment is -0.52 Sv (Figure 5.1b). The standard deviation for the variability of AW volume transport is 0.16 Sv, with an average annual coefficient of variability of 0.35 obtained from 204 monthly AW volume transports. It has been more variable and has increased slightly since 2009, with an interannual coefficient of variability of 0.24 obtained from 17 annual averages of AW volume transport. The annual cycle of AW volume transport has a minimum in the winter or spring and maximum in the latter half of the year. The two flow reversals in AW volume transport are also found in the same periods spanning, so AW volume transport dominates the reversal volume transport at Nares Strait. Total volume transport at Nares Strait is closely related to the AW volume transport with the correlation coefficient of 0.86. The freshwater and heat transport also have strong links to AW volume transport with the correlation coefficient of 0.96 and -0.96. Besides, Both AW and TrW volume transport at Nares Strait contributes to total volume transport, but only AW volume transport has a severe influence on freshwater transport.

The mean AW volume transport of -0.67 is nearly equal to the net volume transport at Barrow Strait (Figure 5.1c), representing it is the main source of the volume transport. Therefore, the AW volume transport shows an extremely similar variability (An average annual coefficient of variability: 0.51; An interannual coefficient of variability: 0.47), and statistically significant correlations with the total volume transport ($r=0.99$), freshwater transport ($r=0.92$) and heat transport ($r=-0.97$).

5.2. Transitional Water

The TrW volume transport at Davis Strait is -0.71 Sv, half of the AW volume transport, making it the second largest component of the total volume transport (Figure 5.1d). The sum of total volume transports at CAA gateway straits into Baffin Bay (-1.87 Sv) takes up 87.8% of the net flow by TrW plus AW at Davis Strait. By comparison with the AW, TrW is more saline ranging from 33.7 to 34.1. In addition, it shows large annual

fluctuations from 2002 to 2006 and remains relatively stable in the later years. The standard deviations for the average of annual TrW volume transport for these two periods are 0.35 Sv and 0.13 Sv. The TrW volume transport hits the trough from 2012 to 2015 with less than -0.5 Sv, followed by a slight recovery in recent years. The interannual variability is large with the coefficient of 0.54.

At Nares Strait, the mean TrW volume transport is -0.37 Sv, and it is the other significant constituent of the net volume transport (Figure 5.1e). The variability of TrW volume transport is larger for the first three years, with an average annual coefficient of variability of 0.32 obtained from 204 monthly TrW volume transports and an interannual coefficient of variability of 0.38 obtained from 17 annual averages of TrW volume transport. It tends to have more flux in the summer and autumn over each year and two low-intensity flow reversals are also observed. TrW volume transport at Nares Strait is correlated to the total volume transport with the correlation coefficient of 0.79, but it does not have close relevance to the freshwater transport. At both Davis Strait and Nares Strait, there exists a kind of connection between the AW and TrW in variability, one would become less variable if the other has lots of variabilities during some years, implying their possibility to invert mutually as well. The contribution to volume transport is insignificantly made by TrW at Barrow Strait, with an average transport of -0.02 Sv (Figure 5.1f). Southward flow only appears and fluctuates in the first two years in the model and then becomes negligible.

5.3. West Greenland Shelf and Irminger Water

The average of WGSW volume transport is 0.30 Sv, flowing northwards into Baffin Bay in general (Figure 5.1g). This represents 11% of the total volume transport from 2002 to 2018 (Figure 5.2a). For most years, the WGSW volume transport is close to zero in the winter and spring and reach at peak in the autumn. Therefore, the annual variability is very high with an average annual variability coefficient of 1.16. There is the highest peak from November 2010 to January 2011, verifying that WGSW plays an important role in the first flow reversal. The interannual variability is large with the coefficient of 0.55.

The WGIW volume transport is at the same magnitude as WGSW, with an average of 0.32 Sv (Figure 5.1j), occupying 12 % of the net volume transport at Davis Strait (Figure 5.2a). WGIW could recirculate and flow southward through Davis Strait, and it becomes more frequent in the spring and summer during recent years since 2012. Overall transport into Baffin Bay is a bit less thereafter. The annual variability is extremely high with an average annual variability coefficient of 8.56. The WGIW volume also reaches its maximal value of about 1.5 Sv during the first flow reversal. In December 2010, both WGSW and WGIW volume transport surpass AW and the sum of them is over the total AW and TrW outflow, resulting in the flow reversal (Figure 5.2c). The second flow reversal in December 2017 is only because of the augmentation of WGIW volume transport. Having a spike of 1.82 Sv is large enough to have a profound effect. The WGIW volume transport has a strong link to the heat transport at Davis Strait ($r=0.91$). The impact of WGIW and WGSW to both Nares Strait and Barrow Strait is marginal, but the peaks imply these two water masses are involved at Nares Strait during flow reversal months.

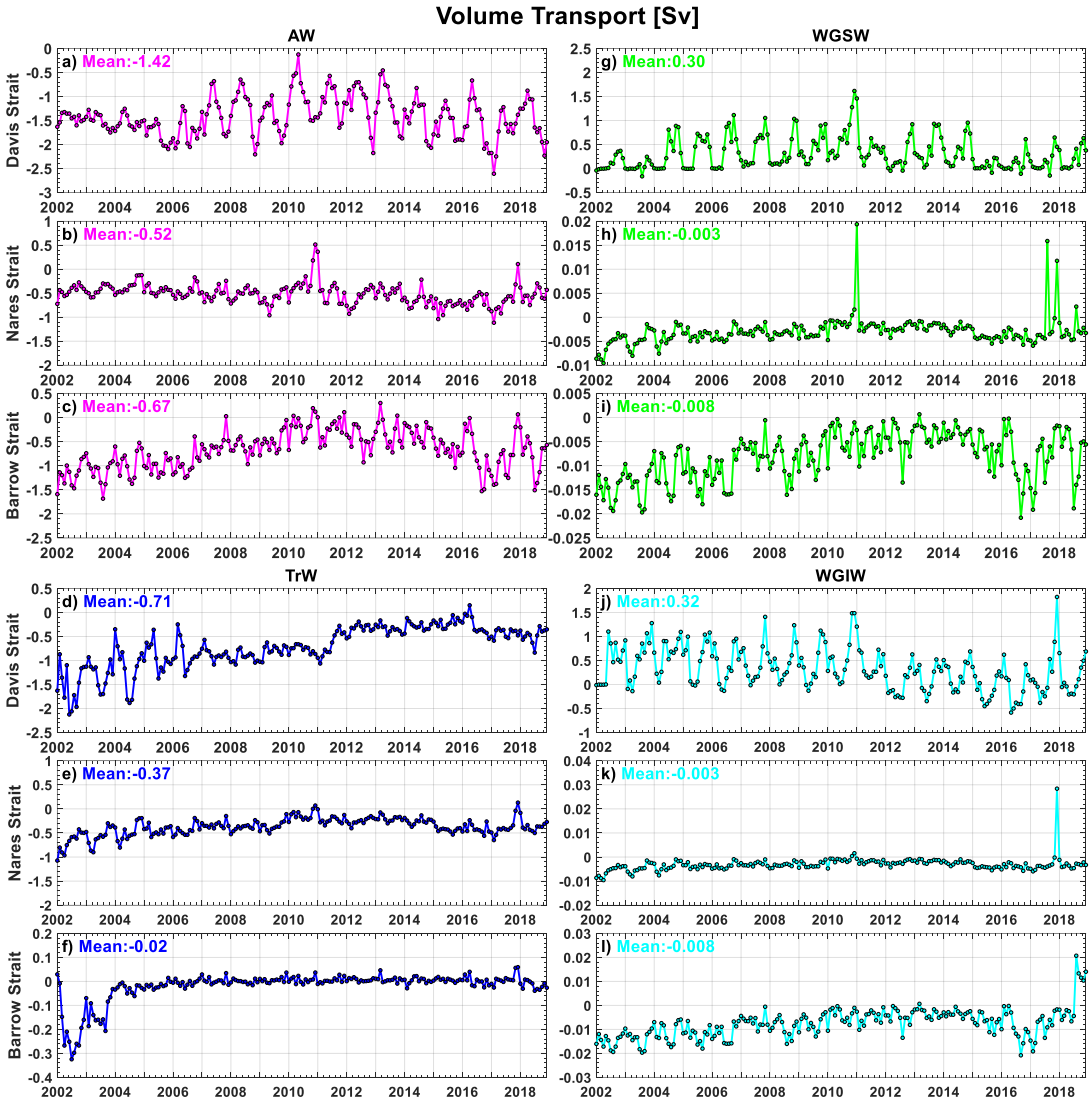

Figure 5.1. Volume transport of water masses (AW, WGSW, TrW and WGIW) through Davis Strait, Nares Strait and Barrow Strait from 2002 to 2018. They are shown on a monthly transport with colored lines (magenta, green, blue and cyan accordingly). Boundaries for the water masses are given in Section 4.1.1. The sign refers to the direction rather than the magnitude, which is prescribed as a positive value means toward the Arctic Ocean, while a negative value means into the North Atlantic, i.e. transports are positive northwards and westwards.

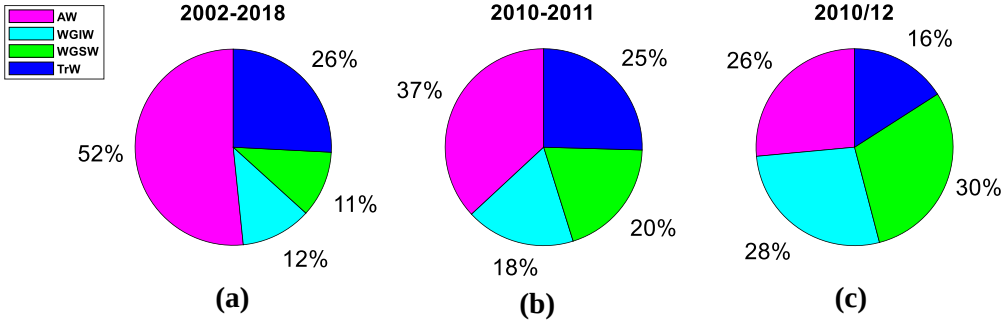

Figure 5.2. Percentages of four water masses (AW, WGSW, TrW, WGIW) through Davis Strait over (a) 2002-2018, (b) 2010-2011 and (c) 2010/12.

6. Contents within Regions (2002-2018)

6.1. Baffin Bay enclosed by the straits

Baffin Bay is deep in the middle and relatively shallow on all sides topographically. The contour of 700 m basically draws clear lines of demarcation between the region with more freshwater and less freshwater (Figure 6.1). This is because deeper region tends to have more seawater and thus contain more freshwater. The freshwater content is particularly concentrated at the entrances of the CAA gateway straits (Western Smith South, Jones Sound and Lancaster Sound), along the slope and in the troughs and fjords of Baffin Island, which as a result improves its buoyancy, density and sea surface height in the upper western Baffin Bay. From July to December, the center of Baffin Bay has more freshwater than the other months. It should be a consequence of the melting sea ice and spreading BIC. The strengthening of WGC and WGSC also leads to the increase of the freshwater on the slope and shelf of Greenland during the summer and autumn. More freshwater accumulates inside the fjords due to the accelerating glacial melting runoff. There is more heat content along the WGC pathway extending to the northern part of Baffin Bay (Figure 6.2). A great amount of heat is entering into the fjords on the Greenland coast through the troughs, warming up the areas and leading to the melting of glaciers. The warming effect is more pronounced during autumn when the WGIW reaches its maximum. More heat inflow through Davis Strait would also lift the sea surface height in eastern region of Baffin Bay because of thermal expansion. The Arctic Water inflows in northern passages almost make no contribution to the heat content in Baffin Bay.

The average of total freshwater content is 8200 km^3 within Baffin Bay for the top 700 m (Figure 6.1a). The freshwater content variability is greatly influenced by the season, indicating the freshwater content is more related to seasonal atmospheric and oceanic temperature changes than the heat content. Both the timings of the yearly minimum and maximum have high consistency from year to year, with the minimum in April and then climb up to the maximum in September or October. The average annual coefficient of variability is 0.05, which is not that large because of the huge freshwater inventory contained in Baffin Bay. The annual average of freshwater content keeps increased steadily during the period from 2002 to 2010, then shows a downward trend thereafter until 2015 but has quite a large drop in 2011. It has a modest recovery in recent years. The interannual coefficient of variability is 0.06.

The freshwater transport through all the gateway straits plays a critical role in revising the freshwater budget of Baffin Bay, whereas only the heat transport through Davis Strait is a key source of the heat storage. The mean heat content is 8.8×10^{10} kJ within Baffin Bay as well for top 700 m (Figure 6.1b). There is no clear trend in an annual cycle except for a noticeable increase in summer. The heat content experiences a significant rise until reaches the plateau in 2010, with a slight peak between 2014 and 2015. Combined with these two figures for analysis, Baffin Bay has become fresher and warmer from 2002 to 2010.

6.2. Baffin Bay Box on the West of Greenland

Baffin Bay is a large deep body of water with access to the North Atlantic Ocean and the Arctic Ocean, so there are quite a lot of factors leading to the change of heat and freshwater content in the region. The scope is reduced to Baffin Bay Box (Figure 6.4a), basically covering troughs, fjords and adjacent waterway passages for WGSC in the vicinity of Davis Strait, whose heat and freshwater contents are mainly affected by the thermohaline intrusion through Davis Strait and glacial meltwater from west Greenland. The variabilities of the freshwater and heat contents within Baffin Bay Box for different integration depths (200m, 500m and entire water column) are represented in Figure 6.4.

For the top 200m surface layer, the averages of freshwater and heat content in the experiment are 695 km^3 and 0.97×10^{10} kJ, respectively (Figure 6.4b). The freshwater content occupies an overwhelming majority of the vertical freshwater distribution in the region. The contribution primarily comes from the accumulated Greenland glacial meltwater in the fjords and the freshwater carried by WGSC over the continental shelf during the summer and autumn, hence the variation of freshwater exhibits strong seasonality each year. The trend is fairly stable in the first several years but becomes fluctuant with larger range for the rest years after 2006. The pattern is opposite for heat content, whereas there exists a marked rise at the end of 2010. The increase is due to the heat contained inside the WGSW and advected from WGIW through the troughs. The water masses are warm and salty, so at the same time they also result in a distinct decline in freshwater content. The added heat is likely to enter the fjords and accelerate glacier melt and retreat gradually. The averages of freshwater and heat content for the top 500m in the Baffin Bay Box are 695 km^3 and 0.97×10^{10} kJ, respectively (Figure 6.4c). The heat content has an obvious increase because of the heat trapped in the troughs at mid-depth. The total amount and variability of freshwater and heat content make no big difference for entire water column (Figure 6.4d).

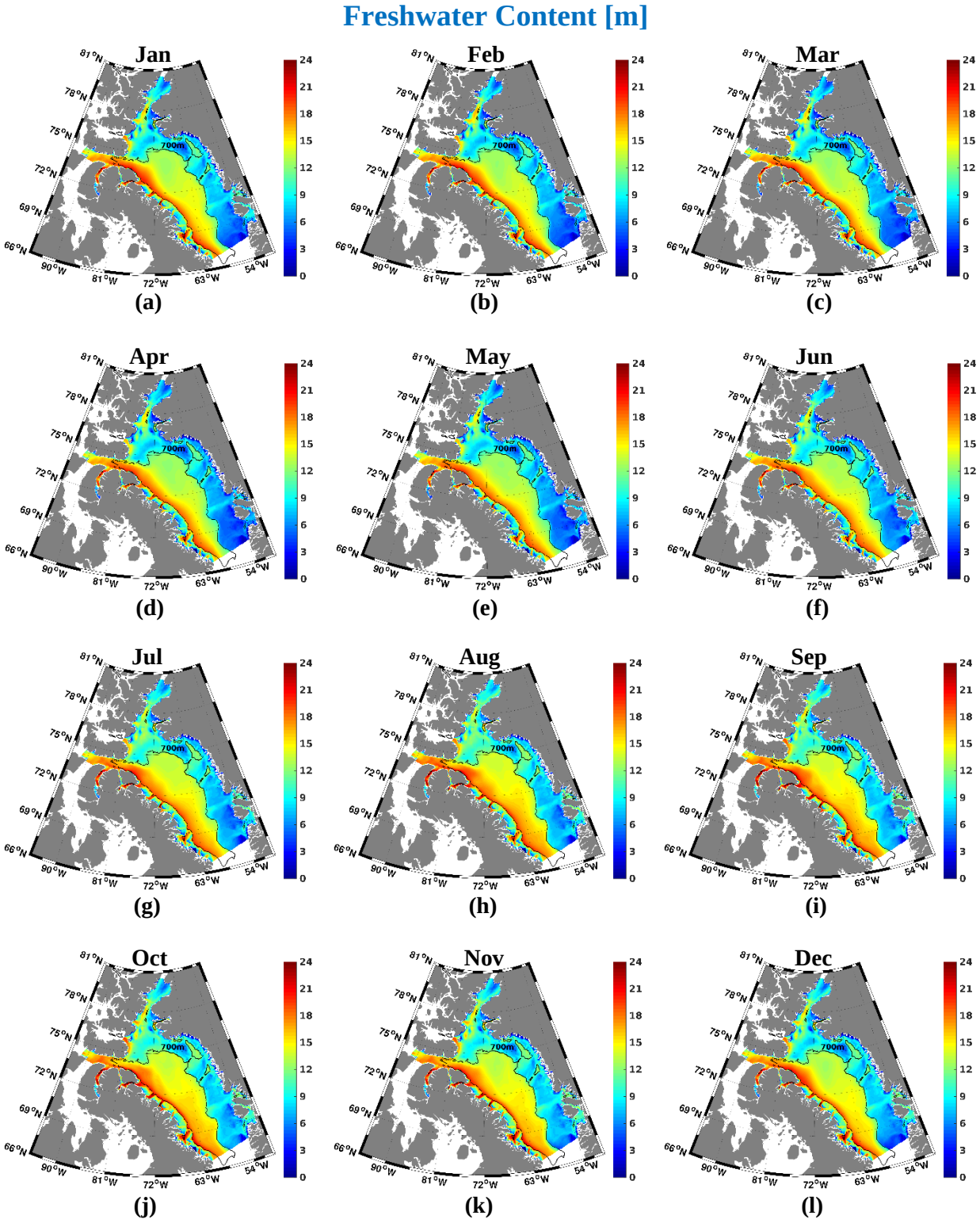

Figure 6.1. Horizontal plotting of the freshwater content in monthly change for the top 700m within Baffin Bay over the time period of 2002 - 2018 - defined the region enclosed by the sections of Davis Strait, Nares Strait and Barrow Strait. The contour of 700 m is shown on the maps. The freshwater content is calculated from the seawater whose salinity is lower than reference 34.8 psu.

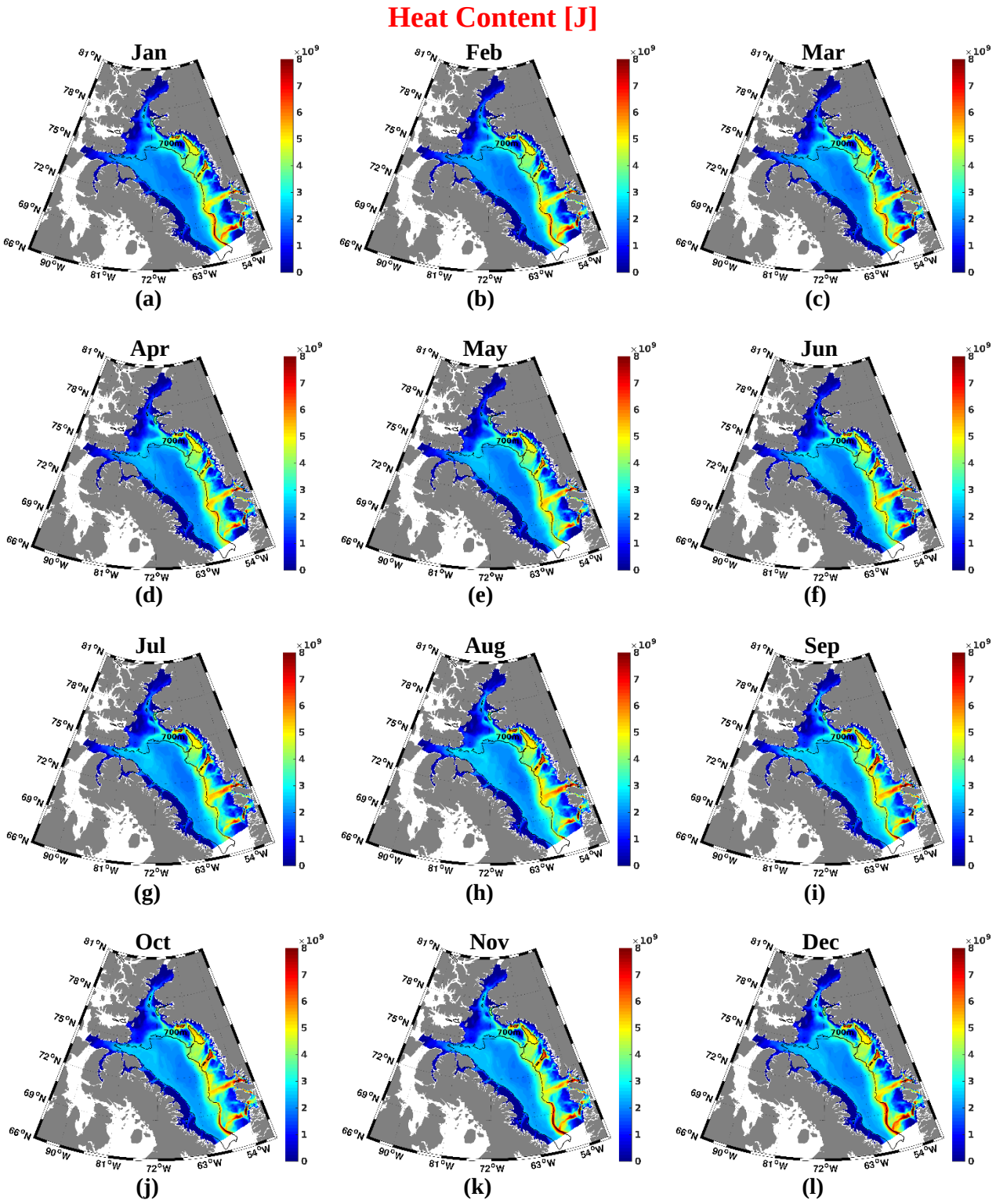

Figure 6.2. Horizontal plotting of the heat content in monthly change for the top 700m within Baffin Bay over the time period of 2002 - 2018 - defined the region enclosed by the sections of Davis Strait, Nares Strait and Barrow Strait. The contour of 700 m is shown on the maps. The heat content is calculated from the seawater whose temperature is above reference 0 ℃.

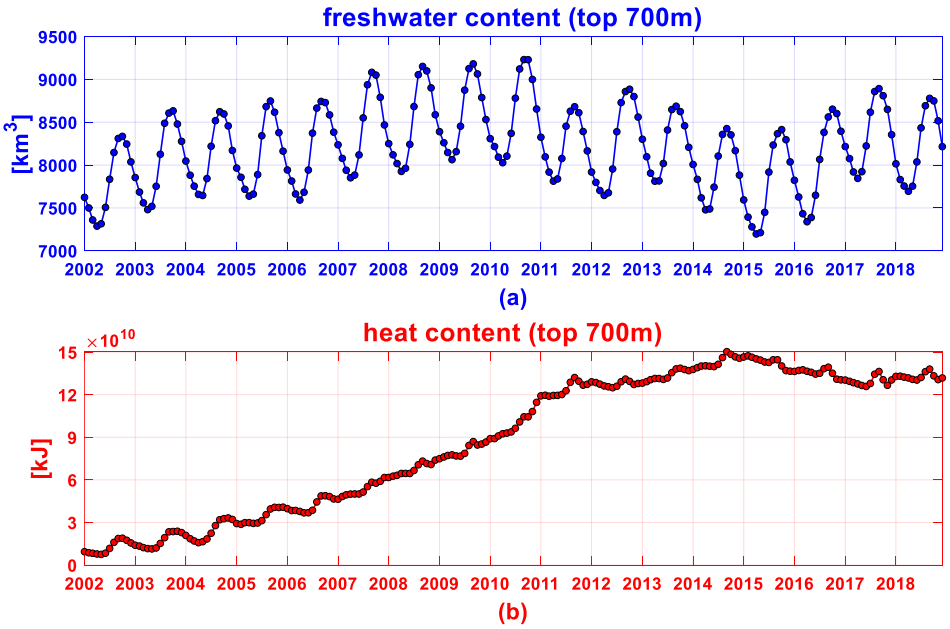

Figure 6.3. The freshwater and heat content for top 700m water column within Baffin Bay, shown on monthly average data from 2002 to 2018.

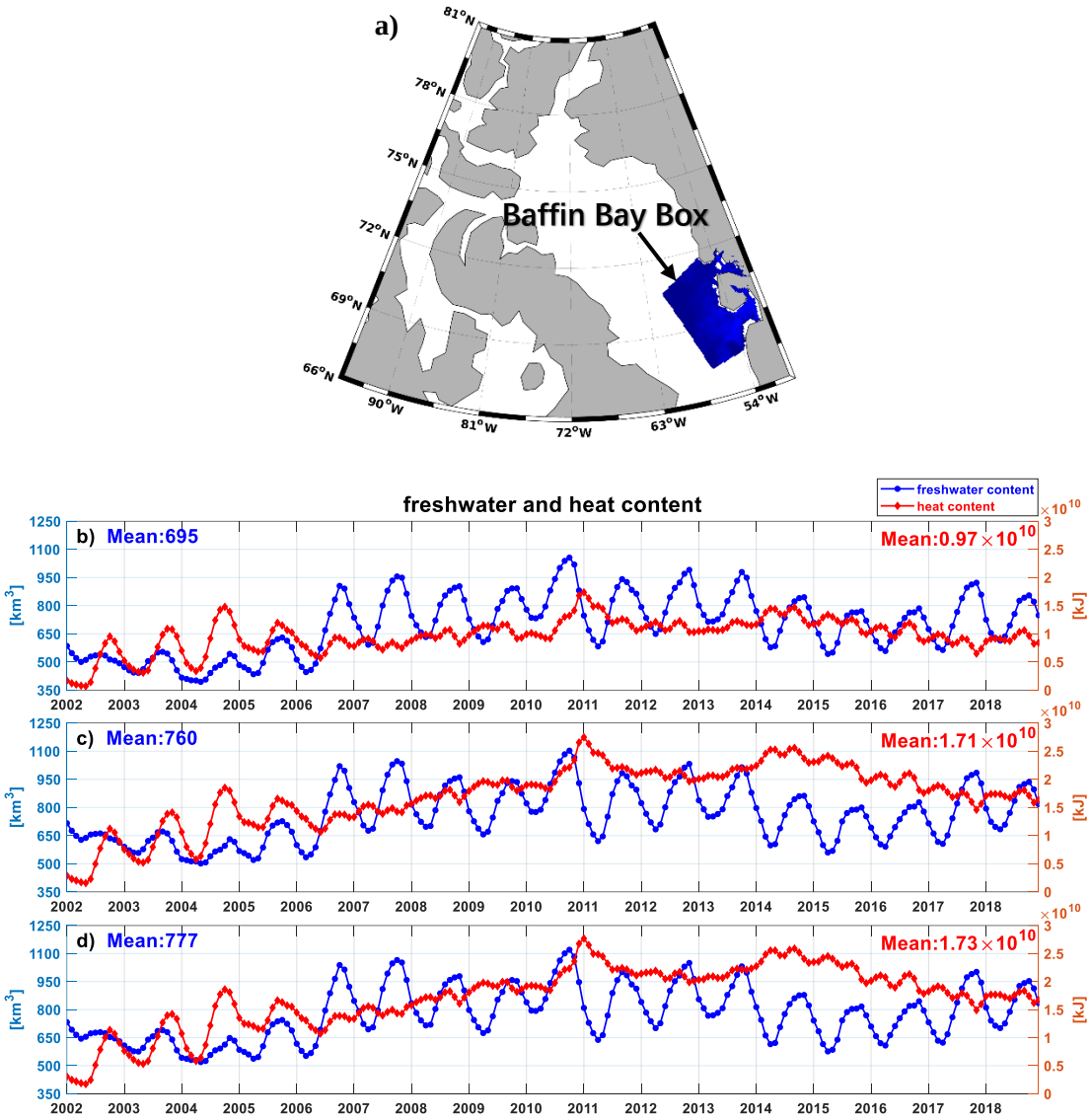

Figure 6.4. The freshwater and heat content within Baffin Bay Box (blue area in (a) highlighted by a black arrow) from 2002 to 2018. They are shown on a monthly basis for top 200m (b), top 500m (c), and entire water column (d). The averages of freshwater and heat content are also presented in each figure.

7. Summary and Conclusions

One valuable work that has been done in this thesis is the comparison between the observational transports from previous studies and the ocean modelling transports using the ANHA12 configuration. They match quite well with each other correspondingly, indicating the validity and accuracy of the ocean model simulation. The heat and freshwater transports are more related to the volume transport in Nares Strait and Barrow Strait than Davis Strait because of the four water masses of distinct physical properties involved. We also find out statistically significant correlations in volume transport between Davis Strait and Nares Strait as well as Barrow Strait, proving the strong link between the northern inflows and Davis Strait net outflow. For the volume transport at Nares Strait, the freshwater transport at Barrow Strait and the heat transport at Davis Strait, they show that the annual variability is greatly larger than the interannual variability.

A large amount of heat and salt carried by WGIW and WGSW comes into Baffin Bay through the east of Davis Strait, while the fresher and colder seawater primarily as AW keeps flowing out on the other side. This process varies because the changes of the water masses show a strong seasonal pattern on an annual cycle. At Davis Strait, first flow reversal was found from November 2010 to January 2011, and it has higher correlations for variability with heat transport than freshwater transport. It is caused by the reinforced northward WGSW and WGIW and diminished southward AW. The second flow reversal was found in December 2017, the leading reason is the exceptional increase in WGIW. At Nares Strait, first flow reversal (AW: 0.5 Sv; WGSW: 0.02 Sv) and Second flow reversal (AW: 0.15 Sv; WGSW: 0.01 Sv; WGIW: 0.03 Sv) over the same periods are the result of a dominated northward AW, which we speculate could be transformed from the northward WGSW and WGIW. It is highly likely that there is a driving mechanism accelerating cyclonical circulation in Baffin Bay, then enhancing the northward flow along the west continental shelf and slope of Greenland, so that these two reversals occurred.

The volume and freshwater transports through the different straits are sensitive to the elevation difference, the density distribution and baroclinic pressure gradients (Kliem and Greenberg, 2003). The study results using the same numerical configuration by Castro de la Guardia, Hu and Myers (2015) also revealed that the elevation difference reduces the Arctic Water inflow through CAA, whereas increases the norward transport across Davis Strait. The strengthening WGC and WGSC contained lots of heat enter the fjords and thus lead to the melting of glaciers. The additional meltwater as a result induces the raising sea surface height in Baffin Bay.

We analyzed three kinds of transport at the gateway straits and evaluated the sensitivity of Baffin Bay to exchanges, but the factors controlling the throughflow is still an open question. For instance, wind surface stress, sea surface height, baroclinic gradient, sea ice concentration and velocity, ice sheet melting and so on. How and to what extent they might relate to the transport in our model needed to be further probed and analyzed.

8. References

Aksenov, Y. et al. (2010) 'Polar outflow from the Arctic Ocean: A high resolution model study'. Elsevier BV, 83(1–2), pp. 14–37. doi: 10.1016/j.jmarsys.2010.06.007.

Bernard, B. et al. (2006) 'Impact of partial steps and momentum advection schemes in a global ocean circulation model at eddy-permitting resolution'. Springer Science + Business Media, 56(5–6), pp. 543–567. doi: 10.1007/s10236-006-0082-1.

Cuny, J., Rhines, P. B. and Kwok, R. (2005) 'Davis Strait volume, freshwater and heat fluxes', Deep Sea Research Part I: Oceanographic Research Papers. Elsevier BV, 52(3), pp. 519–542. doi: 10.1016/j.dsr.2004.10.006.

Castro de la Guardia, L., Hu, X. and Myers, P. G. (2015) 'Potential positive feedback between Greenland Ice Sheet melt and Baffin Bay heat content on the west Greenland shelf', *Geophysical Research Letters*. John Wiley & Sons, Ltd, 42(12), pp. 4922–4930. doi: 10.1002/2015GL064626.

Curry, B. et al. (2014) 'Multiyear volume, liquid freshwater, and sea ice transports through Davis Strait, 2004-10', Journal of Physical Oceanography, 44(4), pp. 1244–1266. doi: 10.1175/JPO-D-13-0177.1.

Curry, B., Lee, C. M. and Petrie, B. (2011) 'Volume, freshwater, and heat fluxes through Davis Strait, 2004-05', Journal of Physical Oceanography, 41(3), pp. 429–436. doi: 10.1175/2010JPO4536.1.

Fichefet, T. and Maqueda, M. A. M. (1997) 'Sensitivity of a global sea ice model to the treatment of ice thermodynamics and dynamics'. Wiley-Blackwell, 102(C6), pp. 12609–12646. doi: 10.1029/97jc00480.

Fissel, D. B., Lemon, D. D. and Birch, J. R. (1982) 'Major Features of the Summer Near-Surface Circulation of Western Baffin Bay, 1978 and 1979', ARCTIC. The Arctic Institute of North America, 35(1). doi: 10.14430/arctic2318.

Grivault, N., Hu, X. and Myers, P. G. (2018) 'Impact of the Surface Stress on the Volume and Freshwater Transport Through the Canadian Arctic Archipelago From a High-Resolution Numerical Simulation', Journal of Geophysical Research: Oceans, 123(12), pp. 9038–9060. doi: 10.1029/2018JC013984.

Hu, X. et al. (2018) 'Thermodynamic and dynamic ice thickness contributions in the Canadian Arctic Archipelago in NEMO-LIM2 numerical simulations', Cryosphere, 12(4), pp. 1233–1247. doi: 10.5194/tc-12-1233-2018.

Hu, X., Myers, P. G. and Lu, Y. (2019) 'Pacific Water Pathway in the Arctic Ocean and Beaufort Gyre in Two Simulations With Different Horizontal Resolutions', Journal of Geophysical Research: Oceans. American Geophysical Union (AGU). doi: 10.1029/2019jc015111.

Hunke, E. C. and Dukowicz, J. K. (1997) 'An Elastic–Viscous–Plastic Model for Sea Ice Dynamics'. American Meteorological Society, 27(9), pp. 1849–1867. doi: 10.1175/1520-0485(1997)027<1849:aevpmf>2.0.co;2.

Kliem, N. and Greenberg, D. A. (2003) ‘Diagnostic simulations of the summer circulation in the Canadian Arctic Archipelago’, *Atmosphere - Ocean*, 41(4), pp. 273–289. doi: 10.3137/ao.410402.

Lu, Y. et al. (2014) ‘Model simulated volume fluxes through the Canadian Arctic Archipelago and Davis Strait: Linking monthly variations to forcing in different seasons’. Wiley-Blackwell, 119(3), pp. 1927–1942. doi: 10.1002/2013jc009408.

Masina, S. et al. (2017) ‘An ensemble of eddy-permitting global ocean reanalyses from the MyOcean project’, Climate Dynamics, 49(3), pp. 813–841. doi: 10.1007/s00382-015-2728-5.

Mesinger, F. and Arakawa, A. (1976) ‘Numerical methods used in atmospheric models, GARP Publication Series, No. 14’, *Global Atmospheric Research Program, World Meteorological Organization, Geneva (Switzerland).*

Münchow, A. (2016) ‘Volume and freshwater flux observations from Nares Strait to the west of Greenland at daily time scales from 2003 to 2009’, Journal of Physical Oceanography, 46(1), pp. 141–157. doi: 10.1175/JPO-D-15-0093.1.

Peterson, I. et al. (2012) ‘Wind-forcing of volume transport through Lancaster Sound’, Journal of Geophysical Research: Oceans, 117(11), pp. 1–17. doi: 10.1029/2012JC008140.

Rabe, B. et al. (2012) ‘Geostrophic ocean currents and freshwater fluxes across the Canadian polar shelf via Nares Strait’. Journal of Marine Research/Yale, 70(4), pp. 603–640. doi: 10.1357/002224012805262725.

Ridenour, N. et al. (2019) ‘Sensitivity of freshwater dynamics to ocean model resolution and river discharge forcing in the Hudson Bay Complex’, Journal of Marine Systems, 196. doi: 10.1016/j.jmarsys.2019.04.002.

Ryan, P. A. (2017) ‘Sea ice draft observations in Nares Strait from 2003 to 2012’, Journal of Geophysical Research: Oceans, 175(4449), p. 238. doi: 10.1038/175238c0.

Samelson, R. M. et al. (2006) ‘Evidence for atmospheric control of sea-ice motion through Nares Strait’, Geophysical Research Letters. American Geophysical Union (AGU), 33(2). doi: 10.1029/2005gl025016.

Samelson, R. M. and Barbour, P. L. (2008) ‘Low-Level Jets, Orographic Effects, and Extreme Events in Nares Strait: A Model-Based Mesoscale Climatology’, Monthly Weather Review. American Meteorological Society, 136(12), pp. 4746–4759. doi: 10.1175/2007mwr2326.1.

Shroyer, E. L. et al. (2015) ‘Modeled ocean circulation in Nares Strait and its dependence on landfast-ice cover’. Wiley-Blackwell, 120(12), pp. 7934–7959. doi: 10.1002/2015jc011091.

Smith, G. C. et al. (2014) ‘A new atmospheric dataset for forcing ice-ocean models: Evaluation of reforecasts using the Canadian global deterministic prediction system’, Quarterly Journal of the Royal Meteorological Society. Wiley, 140(680), pp. 881–894. doi: 10.1002/qj.2194.

Subarctic, A. and Fluxes, O. (2008) Fresh-water fluxes via Pacific and Arctic outflows across the Canadian Polar Shelf, Arctic–Subarctic Ocean Fluxes. doi: 10.1007/978-1-4020-6774-7.

Tang, C. C. L. et al. (2004) 'The circulation, water masses and sea-ice of Baffin Bay'. Elsevier BV, 63(4), pp. 183–228. doi: 10.1016/j.pocean.2004.09.005.

Wang, Q. et al. (2012) 'Flow Constraints on Pathways through the Canadian Arctic Archipelago', Atmosphere-Ocean. Informa UK Limited, 50(3), pp. 373–385. doi: 10.1080/07055900.2012.704348.

Wekerle, C. et al. (2013) 'The Canadian Arctic Archipelago throughflow in a multiresolution global model: Model assessment and the driving mechanism of interannual variability'. Wiley-Blackwell, 118(9), pp. 4525–4541. doi: 10.1002/jgrc.20330.

Zweng, M. M. and Münchow, A. (2006) 'Warming and freshening of Baffin Bay, 1916–2003'. Wiley-Blackwell, 111(C7). doi: 10.1029/2005jc003093.